Pacific Northwest
NATIONAL LABORATORY

PNNL-36689

Accelerating the identification of novel secondary metabolites in bioenergy plant root exudates using MicroED

September 2024

Samantha M. Powell
Daisy Herrera
Irina El Khoury
Cayden M. Perdue
Natalie C. Sadler
John R. Cort
Grace O. Robinson
Pubudu Handakumbura
James F. Evans
Vivian S. Lin

U.S. DEPARTMENT OF ENERGY

Prepared for the U.S. Department of Energy
under Contract DE-AC05-76RL01830

DISCLAIMER

PACIFIC NORTHWEST NATIONAL LABORATORY
operated by
BATTELLE
for the
UNITED STATES DEPARTMENT OF ENERGY
under Contract DE-AC05-76RL01830

Printed in the United States of America

Available to DOE and DOE contractors from
the Office of Scientific and Technical Information,
P.O. Box 62, Oak Ridge, TN 37831-0062
www.osti.gov
ph: (865) 576-8401
fox: (865) 576-5728
email: reports@osti.gov

Available to the public from the National Technical Information Service
5301 Shawnee Rd., Alexandria, VA 22312
ph: (800) 553-NTIS (6847)
or (703) 605-6000
email: info@ntis.gov
Online ordering: http://www.ntis.gov

PNNL-36689

0BAccelerating the identification of novel secondary metabolites in bioenergy plant root exudates using MicroED

September 2024

Samantha M. Powell
Daisy Herrera
Irina El Khoury
Cayden M. Perdue
Natalie C. Sadler
John R. Cort
Grace O. Robinson
Pubudu Handakumbura
James F. Evans
Vivian S. Lin

Prepared for
the U.S. Department of Energy
under Contract DE-AC05-76RL01830

Pacific Northwest National Laboratory
Richland, Washington 99354

Abstract

Small molecule metabolites drive inter- and intraspecies communication and dependencies in diverse biological systems, yet a large proportion of these important chemical compounds remain uncharacterized in plants and microbes. Approximately 90% of the metabolites in root exudate profiles are unknown compounds, despite the importance of root exudate composition in plant-microbe interactions. We need advanced analytical capabilities that will support rapid discovery and structural elucidation of metabolites from biological samples that may be limited in quantity and high in complexity. To fill this gap, this project aimed to develop an integrated workflow involving metabolite extraction, separation, and crystallization from plant root exudates followed by characterization using nuclear magnetic resonance (NMR) spectroscopy, mass spectrometry, and microcrystal electron diffraction (MicroED). Using crude root exudates from sorghum, this project successfully developed higher throughput exudate fractionation strategies to obtain pure compounds for crystallization and identified crystals in multiple fractions that diffracted. Additional efforts to increase the throughput of high-quality crystal generation for MicroED, such as crystallization screening and crystallization chaperone exploration, will be needed to further advance root exudate metabolite identification. The overall optimized sample preparation process can then be integrated with the existing data collection and data analysis pipelines for MicroED at PNNL to facilitate more rapid natural product discovery.

Summary

This project developed a workflow for plant root exudate metabolite isolation and identification, encompassing plant growth, exudate extraction, metabolite purification, and chemical characterization. The final workflow utilized methods for higher throughput processing of these highly complex samples, facilitating improved sample fractionation and metabolite isolation. We investigated a combination of nuclear magnetic resonance (NMR) spectroscopy, mass spectrometry (MS) and microcrystal electron diffraction (MicroED) for structural elucidation of metabolites from sorghum root exudates. We obtained the first crystal structure of sorgoleone up to C10 of the alkyl tail, and we obtained complete 1H-NMR shifts for a related compound, 4,6-dimethoxy-2-[(8‘Z,11‘Z)-8‘,11‘,14‘-pentadecatriene]resorcinol, which were incorrectly reported in the literature. We isolated many additional metabolites that could be crystallized and showed diffraction under initial low throughput crystallization, highlighting the potential for this workflow to advance metabolite identification from complex biological samples at PNNL. Our initial investigation of crystallization screening has yielded improved crystal quality over manual, low throughput methods, suggesting that further optimization of crystallization methods will improve the overall quality of samples for MicroED analysis in the future.

Acknowledgments

We are grateful to David Delgadillo and Professor Hosea Nelson at Caltech for their advice regarding metabolite isolation and ArrayED collaboration. We also thank Priscila Lalli, Adam Hollerbach, and Kai-For Mo for help with mass spectrometry analyses; Chathuri Kombala for testing crystallization chaperones; and Phong Huynh for assisting with root exudate extracts. We are grateful to Bob Bickler at Biotage for his advice regarding separation strategies for complex natural product mixtures.

This research was supported by the Open Call Initiative, under the Laboratory Directed Research and Development (LDRD) Program at Pacific Northwest National Laboratory (PNNL). PNNL is a multi-program national laboratory operated for the U.S. Department of Energy (DOE) by Battelle Memorial Institute under Contract No. DE-AC05-76RL01830.

Acronyms and Abbreviations

COSY	Homonuclear correlation spectroscopy
CryoEM	Cryo-electron microscopy
DCM	Dichloromethane
ENACT	Encapsulated nanodroplet crystallization
EtOAc	Ethyl acetate
g	Gram(s)
HMBC	Heteronuclear multiple bond correlation
HPLC	High performance liquid chromatography
HRMS	High-resolution mass spectrometry
HSQC	Heteronuclear single quantum coherence
L	Liter
LC	Liquid chromatography
MeCN	Acetonitrile
MicroED	Microcrystal electron diffraction
mL	Milliliter
MS	Mass spectrometry
NMR	Nuclear magnetic resonance
SiO2	Silica gel
TEM	Transmission electron microscopy
TLC	Thin layer chromatography

Contents

Figures

1.0 Introduction

Immense chemical diversity exists in nature, evolving out of the distinct molecular interactions between small molecules and biological macromolecules produced across all kingdoms of life, from bacteria to fungi, plants, and more. This tightly intertwined relationship between natural product structure and influence on specific biomolecular functions has been exploited for drug discovery and biosystems design and continues to be a source of chemical novelty. However, mining natural sources of chemical diversity such as plant and microbial systems remains a logistical and analytical challenge to the DOE BER community due to the high complexity of these samples.

Plants, which convert some of the simplest molecular carbon building blocks on Earth into exquisitely complex organic structures, interact with a specific subset of the soil microbiome to obtain nutrients, outcompete other plants, and withstand both abiotic and biotic stressors such as drought and pathogenic insult. Plant-microbe interactions are thought to be strongly influenced by root exudate composition, yet ~90% of root exudate metabolite profiles consist of unknown or unidentified organic compounds. Mass spectrometry analyses, while highly sensitive, often observe masses that cannot be assigned to any known structure or are assigned to multiple possible structures. Identifications are therefore frequently limited to well-characterized and highly abundant components, often primary metabolites such as sugars, amino acids, and nucleotides. Thus, a major gap to understanding how plants drive beneficial root-associated (rhizosphere) microbial community assembly and dynamics is this overall scarcity of metabolite annotation, especially for secondary metabolites in root exudates. Predicting and/or controlling specific plant-microbe interactions may depend upon metabolites that are unique to a specific plant host and growth condition, rather than the abundant primary metabolites which we can already identify and are shared amongst most plant species. Approaches that facilitate novel small molecule discovery, in particular *de novo* methods, will help us elucidate the complex biochemical interactions between plant hosts and their associated microbiomes, thereby expanding our opportunities to shape plant-microbial ecosystems through biological design. We envision the workflow developed in this project will also be readily extended to other biological systems producing similarly diverse profiles of natural products to understand the potential impact of these chemical compounds on their native or non-native systems.

1.1 Plant root exudates

Plant root exudation includes both primary metabolites, such as amino acids, carbohydrates, and lipids required for growth and development, as well as secondary metabolites, which are non-essential for growth and development.[1, 2] Root exudation involves the production and transport of organic small molecules from root cells, which facilitate their release into the rhizosphere. Secondary metabolites in root exudates can influence cellular signaling in other organisms, such as bacteria and fungi in the rhizosphere, as well as other plants. These interactions can be beneficial or symbiotic, such as recruiting plant growth promoting bacteria to the rhizosphere, or defensive, such as antifungal or antibacterial functions or inhibiting the growth of competing plants.

Previous mass spectrometry-based metabolomics analyses of sorghum root tissue identified a variety of primary and secondary metabolite compounds, including amino acids such as phenylalanine and tyrosine; hydroxycinammic acids such as coumaric acid, ferulic acid, and sinapic acid; and flavonoids and flavones such as naringenin, galangin, and vitexin. Notably,

most previous metabolomics analyses of sorghum root exudates have focused on polar metabolites, although lipidomics studies have been able to identify more of the nonpolar metabolites.[3]

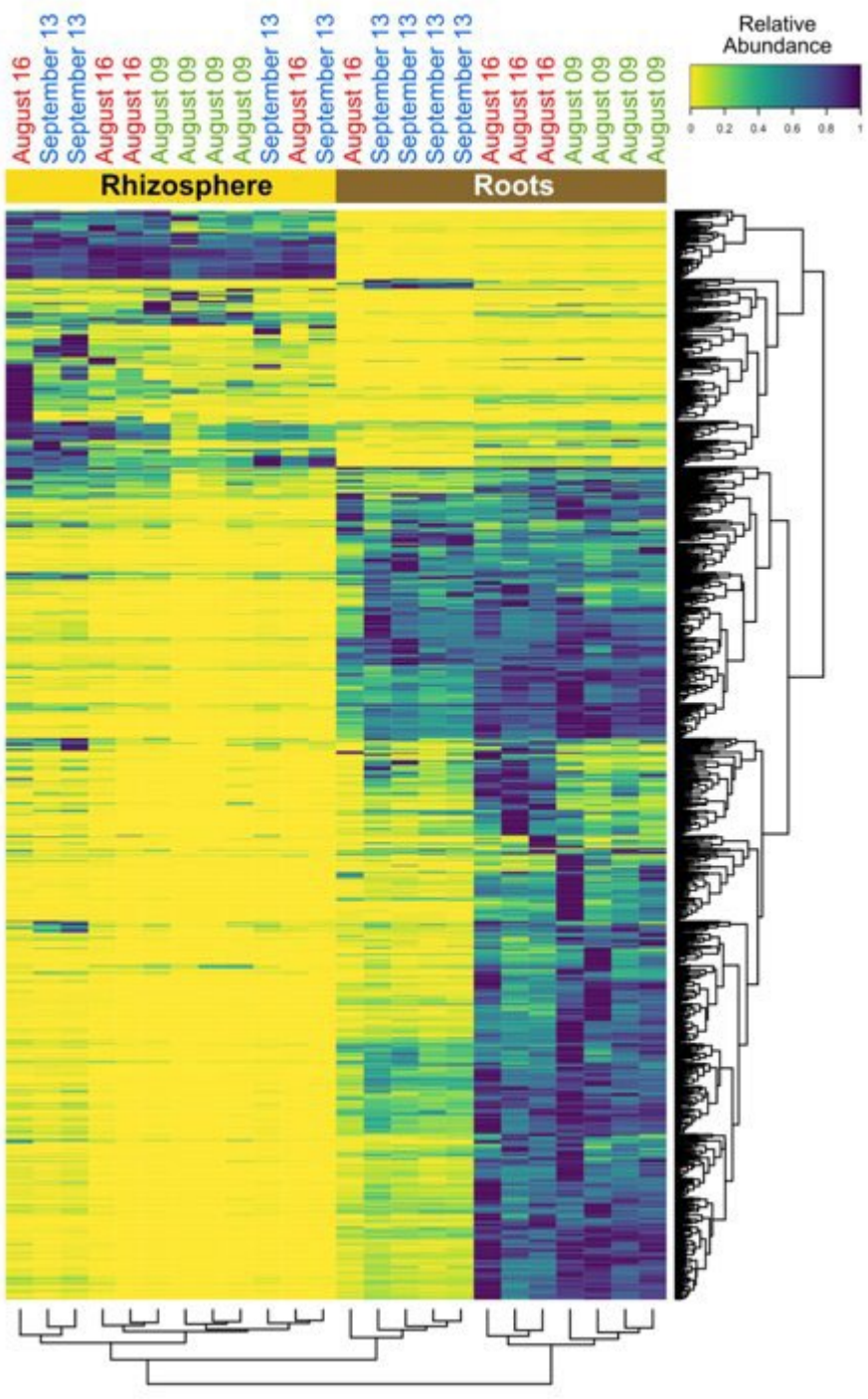

Figure 1. Metabolites identified from roots and rhizosphere of the sorghum BTx642 genotype after 8, 9, and 13 weeks of growth during the Epigenetic Control of Drought Response in Sorghum (EPICON) project field trial.

1.2 Root exudate metabolite isolation and characterization strategies

The isolation of natural products for structural characterization has traditionally relied upon very large starting quantities of material and repeated extraction and purification steps to obtain sufficiently pure material for analysis.[4] Since root exudates are secreted from cells on the outer part of the root into the external environment, the collection of root exudates is relatively straightforward through washing with different solvents, although metabolites may partition into different fractions depending upon their properties, e.g. hydrophobic vs. hydrophilic.

A variety of analytical techniques have been employed for natural product chemical characterization, with nuclear magnetic resonance (NMR) spectroscopy and high-resolution mass spectrometry (HRMS) among the most widely used approaches.[5, 6] NMR is a powerful tool for structure elucidation but requires relatively large quantities of pure substances, making analysis challenging for limited samples. While MS is highly sensitive and provides the chemical formula for a metabolite, compound identification depends upon reference libraries, and most standard MS techniques cannot provide detailed structural information. Additionally, due to the sensitivity of MS instrumentation, MS data can report on strongly ionizable but trace compounds in samples, including contaminants, which may obscure other analytes that are highly abundant but display poor ionization.

Electron diffraction methods have existed for many years, but the term microcrystal electron diffraction (MicroED) was introduced in 2013.[7] MicroED allows for diffraction patterns on thin 3D crystals to be collected while the crystal is continuously rotated and coming of the diffraction patterns results in a 3D structure of the crystallized compound. The advantage of MicroED over other analogous structural techniques is that very little sample needs to be used, and micro and nanocrystals can be used. This is very important when using exudate fractions as there is often limited sample availability. Additionally, multiple samples can be placed across the same grid and the electron beam focused on each crystal individually, making MicroED a more high-throughput technique. These characteristics make MicroED the ideal structural technique to incorporate into a metabolite identification workflow and in fact, a similar workflow has been demonstrated previously.[8] Here, we are looking at a much more complex system (plant root exudates) and have incorporated many more screening steps across all aspects of the workflow (Figure 2).

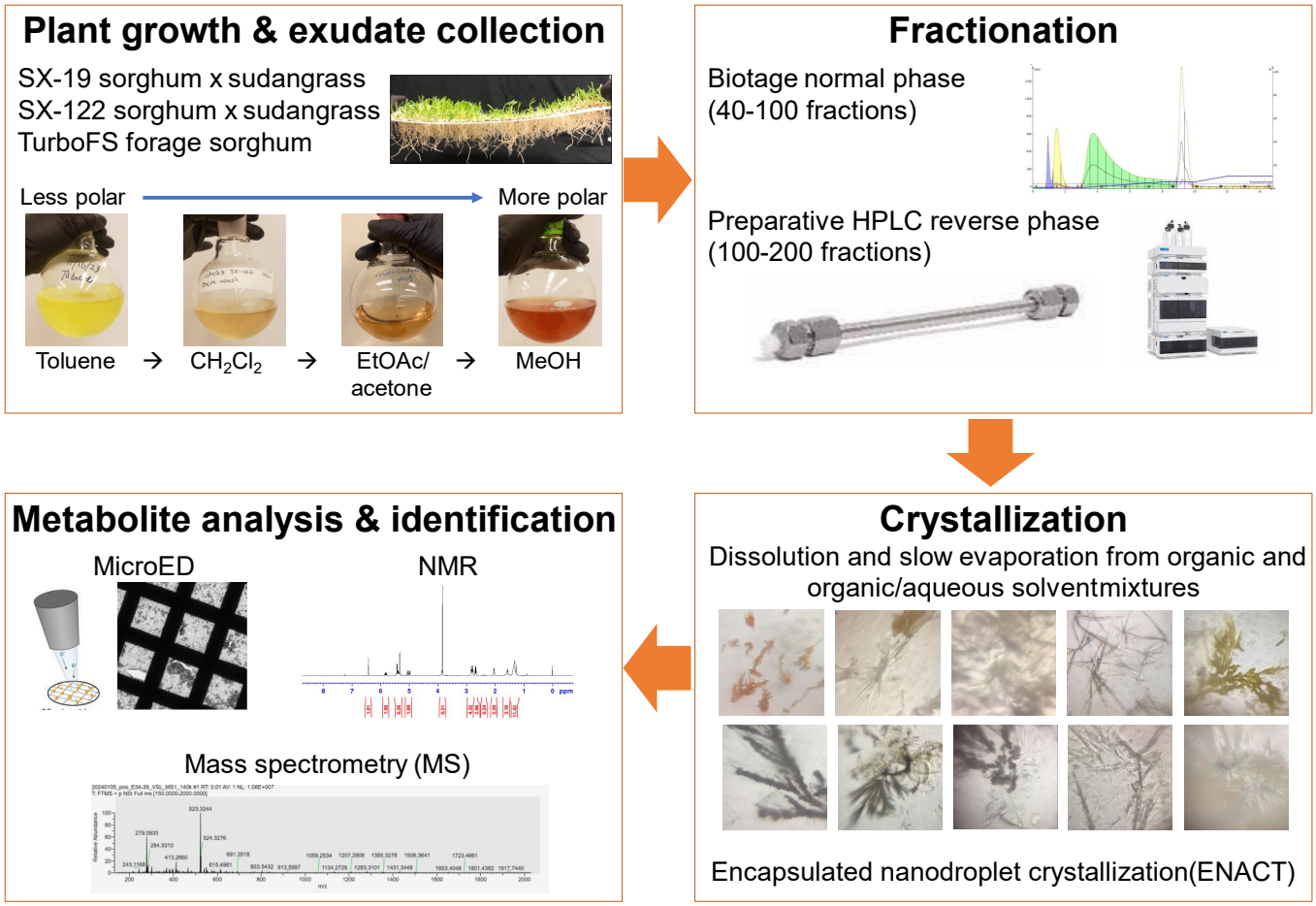

Figure 2. Overall workflow for secondary metabolite isolation and identification from plant root exudates.

2.0 Methods

2.1 Materials

ACS or HPLC grade solvents were purchased and used without further purification from Fisher or VWR. Sudangrass x sorghum SX-19 and SX-122 seeds (Forage Genetics) were purchased from Helena Agri-Enterprises. Forage sorghum Turbo FS 310 seeds were purchased from Sustain Seed + Soil (previously Center Seeds).

2.2 Seed germination and plant growth

Sorghum seeds were germinated and grown on sterile trays for 7-11 days before root harvesting and subsequent exudate collection. To improve the growing conditions of the sorghum seeds of interest, 1,365 g of sorghum seeds were stratified for a minimum of 24 hours in a fridge at 4 °C. This process allows the seeds to experience a dormancy period, mimicking a winter season. When germinating Turbo FS seeds, the seeds were sterilized with 10% bleach concentration in Milli-Q water. The seeds were placed in a 5 L glass beaker and soaked in the 10% bleach solution for 10 minutes while gently agitating. The solution was removed following the appropriate waste disposal methods and the seeds were rinsed up to 8 times with Milli-Q water or until the rinse water was no longer cloudy. There is no sterilization or pretreatment of SX-19 or SX-122 because they are coated in fungicide and herbicide. The beaker was filled with 1.5 L of fresh MilliQ water. All seed strains were soaked for a minimum of 3 hours before planting. This initiates the germination process. All materials used to plant were sterilized by autoclaving at a gravity cycle of 30 minutes minimum. Materials used for planting were Patterson Development trays, mesh plastic canvases, 50 mL tubes, paper towels, and aluminum foil sheets. Paper towels and foil sheets were cut to fit the trays. The materials were allowed to cool after autoclaving. Excess water from the seed soak was poured off and disposed of using the proper waste disposal methods. The laminar flow hood was used during tray set up to maintain sterile conditions.

The following planting procedure workflow is seen in Figure 3. The bottom of a tray was lined with 2 sterile paper towels (Figure 3A-B). Then, 8 sterile 50 mL tubes in 4 sets of two tubes inserted together and laid horizontally onto the tray Figure 3C). The 4 rows of tubes were used to prop up the mesh canvas (Figure 3D). Approximately 130 g of seeds were spread onto the mesh canvas, ensuring that seeds were pushed to the edge and evenly spread (Figure 3E-F). Seeds were then covered with another 4 sheets of sterile paper towels and watered with 250 mL of sterile water (Figure 3G). A sterile aluminum foil sheet was used to cover the tray and pinched in around the sides to seal the tray (Figure 3H). One batch of seeds produced 10-12 trays depending on how well the mesh canvas space was utilized and its size. Trays were kept in a dark growth chamber, at 25°C and >60% humidity until harvest. Every other day, trays would receive an additional 100 mL of sterile water to maintain moisture and receive occasional misting with a sterile water spray bottle. All glassware, gloves, and surfaces were cleaned with 70% ethanol before use.

The roots were harvested by removing the aluminum foil and paper towels that lined the top of the mesh canvas. The mesh canvas was lifted from one end to expose the roots. Using sterile scissors cut the roots as close to the mesh canvas as possible. The roots will fall onto the tray below (Figure 3I). After all the roots are cut from the mesh canvas the roots were placed into a glass beaker using sterile forceps (Figure 3H). Once all trays were collected, the roots were taken to the fume hood for chemical extractions.

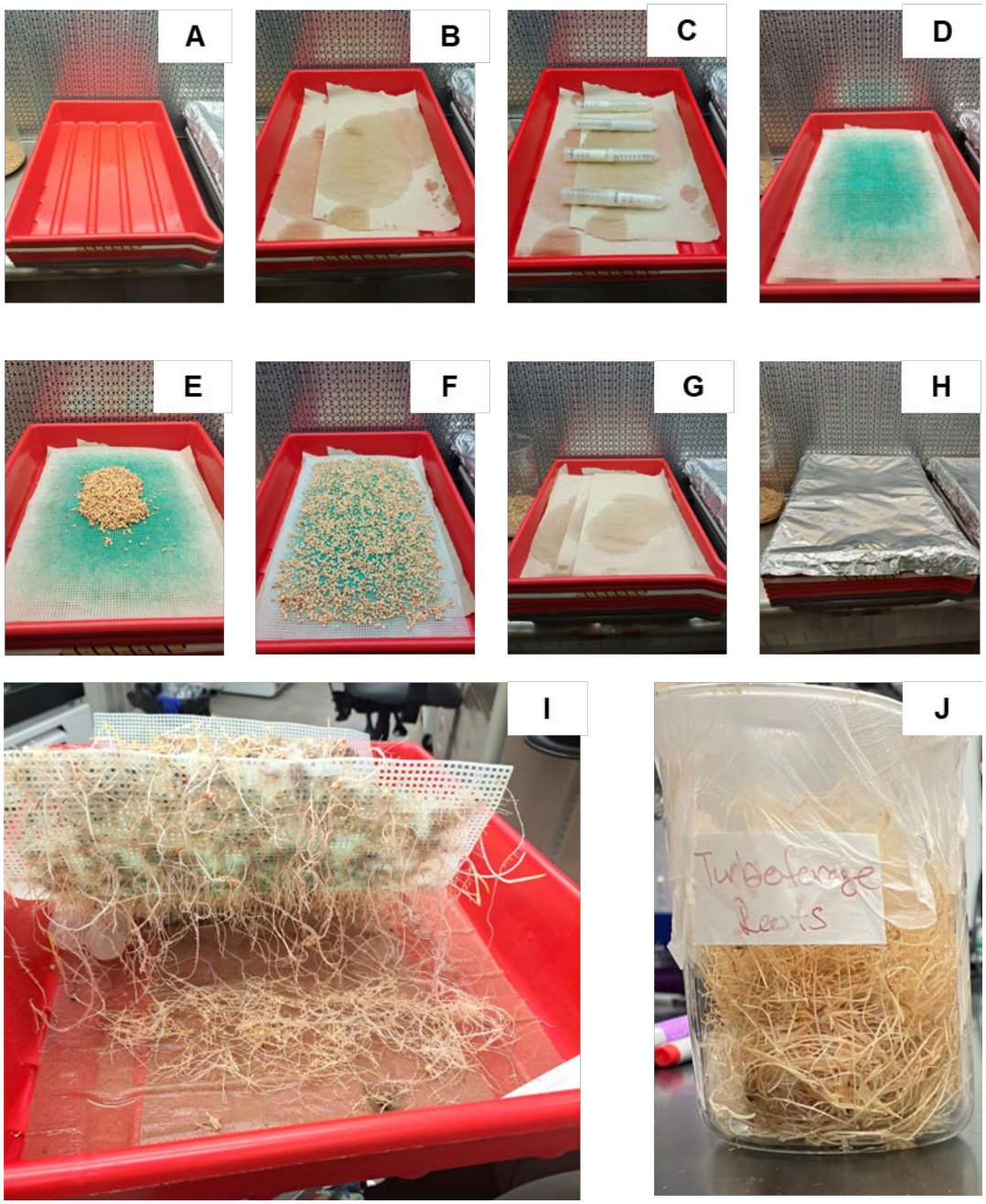

Figure 3. Seed germination and root harvesting workflow. Turbo FS seeds and seedlings are shown. (A) Empty sterile tray. (B) Two paper towels are laid down. (C) Eight 50 ml tubes laid out. (D) Mesh canvas placed atop 50 ml tubes. (E) 130 g seeds added to canvas. (F) Seeds spread out. (G) Four paper towels on top, 250 mL sterile water added. (H) Tray sealed with aluminum foil sheet. (I) Removal of roots during harvest. (J) Turbo FS roots post collection.

2.3 Root exudate extract preparation

Excised roots were washed sequentially with 3x toluene, ethyl acetate, dichloromethane, and methanol, to obtain crude extracts of metabolites in order of increasing polarity. Extracts were stored in diluted form (200-300 mL volume) at 4 °C until ready for chromatography. Storing extracts in concentrated form even at -20 °C led to suspected metabolite degradation due to sample complexity, as noted by a dramatic decrease in recovered yield of the known sorghum metabolite, sorgoleone. Immediately prior to exudate fractionation, solvents were removed by rotary evaporation; heating of toluene and methanol extracts up to 50 °C to evaporate solvents was typically required.

2.4 Root exudate fractionation

Crude root exudate purification was performed using a Biotage Isolera automated flash chromatography system. Normal phase separations were performed using pre-packed SiO_2 columns (12 or 25 g, Luknova or Silicycle), eluting 1-10% MeOH/CH_2Cl_2 or 0-95% EtOAc/hexane. Reverse phase chromatography was performed using Biotage Sfär C18 Duo Reversed Phase pre-packed columns (12 g), eluting 5-95% MeCN/H_2O with 0.1% trifluoroacetic acid.

High performance liquid chromatography (HPLC) was performed using an Agilent Infinity II 1260 HPLC equipped with a preparative C18 5 µm SunFire™ 10 x 150 mm column (Catalog #: 186002563). Concentrated crude exudates were dissolved in a minimal amount of solvent—typically DMSO, methanol, and/or water—and filtered through a 0.22 µm PTFE filter to remove particulates. Samples were loaded into LC vials, and 100-150 µL sample were injected for each run. HPLC separations were performed eluting with water + 0.1% formic acid (FA) and acetonitrile + 0.1% FA. Samples were fractionated over gradients ranging from 5- to 30-95% MeCN/H_2O + 0.1% FA gradient for different extracts.

HPLC fractions were collected in a time-based manner into 16x100 mm glass test tubes (low throughput method) or glass-coated 96-well 1 or 2 mL deepwell plates (Thermo Scientific SureSTART™ WebSeal™ Plate+; high throughput method).

2.5 Low-throughput crystallization

Following fractionation into test tubes, solvents were allowed to evaporate in a fume hood from the glass tubes they were collected in. After 2-4 weeks, crystals formed in the bottom of some of the tubes. Tubes were visually inspected for crystal formation using a low-cost smartphone microscope with glass bead lens (https://www.pnnl.gov/available-technologies/pnnl-smartphone-microscope).

Crystals were scraped from the bottom of the glass tubes or resuspended in a small amount of water/solvent and deposited onto TEM grids (Quantifoil Cu 4/1, 300 mesh). To potentially increase crystal quality, dried down fractions were recrystallized. A small amount of sample was placed in a glass vial and resolubilized using varying solvents and concentrations. The solubilized compound was applied directly to a TEM grid and the solvent was allowed to evaporate, allowing for recrystallization of the compound on the grid. Alternatively, the

solubilized compound was left in the glass vial as the solvent evaporated. As above, formed crystals were scraped from the vial and applied to a TEM grid. In all cases, grids were frozen in liquid nitrogen immediately before CryoEM imaging.

2.6 High-throughput crystallization and screening

To increase the throughput for identifying exudate fractions that are crystalline, we collaborated with Professor Hosea Nelson's group at the California Institute of Technology (Caltech). In our hands, the exudate was HPLC fractionated into 96-well plates (1-2 mL deepwell). Subsequently, 200 µL of each well was transferred into glass-coated 96-well plates (300 µL). All 96-well plates were covered with Breathe-Easier permeable membranes and dried down using a ThermoFisher SpeedVac SPD140P1 concentrator. Plates were covered with aluminum plate sealers and stored at -20 °C. The subsampled 96-well plate was then sent to Caltech for array electron diffraction (ArrayED)[9] to identify which of the 96 fractions diffract using MicroED. The deepwell plates containing the bulk of each fraction were reserved at PNNL for additional analyses.

Solid material from deepwell plates was redissolved in MeCN/H_2O mixtures (< 1 mL) and transferred into 10 x 100 mm glass test tubes. If needed, tubes were gently warmed with a heat gun to ensure full dissolution of solids and/or filtered through 0.22 µm PTFE filters to remove any particulates. Solvent was allowed to slowly evaporate at ambient temperature.

For screening of multiple crystal conditions, we utilized the Encapsulated Nanodroplet Crystallization of Organic-Soluble Small Molecules (ENACT) method.[10] To optimize the ENACT process for generating and harvesting crystals for MicroED, we performed ENACT screening on pure, commercially available salicylic acid, naringenin, quercetin, and tricin, using ethanol and water as solvents in various ratios. Analyte solutions were filtered through a 0.22 µm PTFE filter to remove any particulates. Four types of oils were investigated: Fluorinert FC-40, mineral oil, silicone oil, and Fomblin YR-1800 (in order of increasing viscosity). Rainin micropipettors were used to deliver oils and sample to wells. Initial ENACT testing was performed using 0.9 µL of each oil and 0.12 µL of each sample dissolved in solvent. Both Laminex 100 µm plates and polystyrene 96-well glass-bottom plates were used for initial small-scale tests. Scale up of ENACT samples was performed in polystyrene 96-well glass-bottom plates using 5 µL oil and 1 µL sample volumes or 8-35 µL oil and 5 µL sample volumes.

2.7 Root exudate characterization

2.7.1 Nuclear magnetic resonance (NMR) spectroscopy

NMR characterization was performed on the "Badger Mountain" Bruker 400 MHz Aeon Avance III magnet with BBFO 5 mm probe or the "Mt. Adams" Varian 500 MHz magnet. Samples were dissolved in deuterated solvent ($CDCl_3$, MeOD) and analyzed by 1D-NMR experiments (1H, 13C) and 2D-NMR experiments (COSY, HSQC, HMBC).

All chemical shifts are reported in the standard notation of parts per million using the peak of the residual protonated solvent for $CDCl_3$ (δ 7.24 ppm) or MeOD (δ 4.78 ppm) as an internal reference. Splitting patterns are indicated as follows: s, singlet; d, doublet; t, triplet; m, multiplet; dd, doublet of doublets.

2.7.2 Mass spectrometry

Compound masses were determined using several different mass spectrometers: direct infusion of sample into a Thermo LTQ Orbitrap XL, direct infusion of sample onto a dual-gated structures for lossless ion manipulations (SLIM)-Orbitrap[11], or liquid chromatography mass spectrometry (LC-MS) using a QExactive with Thermo Hypersil GOLD column (2.1 × 150 mm, 3 µm) or QExactive HF with Waters ACQUITY UPLC BEH HILIC column (2.1 × 100 mm, 1.7 µm). Data files (.RAW) were processed using XCalibur software.

2.7.3 MicroED

Microcrystal electron diffraction (MicroED) data was collected on a Thermo-Fisher Titan Krios G3i cryo-transmission electron microscope operating at 300 kV equipped with a Ceta-D CMOS camera. EPU-D (Thermo Fisher Scientific) was used for all data collection. Multiple grids (up to 10) were loaded via autoloader and a low mag atlas was taken for each grid, allowing for visualization of all crystals on the grid without exposing crystals to large amounts of dose. Once a gridsquare with ideal crystals was identified, EPU-D's autoeucentric height function was used to find eucentric height. After locating a crystal, a selected area (SA) aperture was used, limiting the data collection area. Eucentric height of the crystal was further refined manually to ensure that it stayed within the SA aperture for most of the tilt range. An initial diffraction pattern (1 s exposure) was taken to assess crystal quality. The position (x, y, z) of quality crystals was added to a queue for batch data collection. This process was repeated for multiple crystals across the same gridsquare. Using batch collection, data was collected on all saved crystals, by continuously rotating the stage from -65° to +65° at a tilt rate of 0.6°/frame and individual frames were saved as MRC files. This same process was repeated for each gridsquare containing crystals. Data was collected using 1 s exposures at 0.008 e-/Å^2/frame and camera length of 430 or 540 mm. All data was processed using our in-house built software, AutoMicroED.[12]

3.0 Results

3.1 Root exudate isolation

Root exudate crude extracts for 3 different types of sorghum were readily obtained after washing in organic solvents (Figure 4). Initial exudate extractions were performed using only chloroform and methanol, but we determined that increasing the number of solvents and their range of polarities would generate lower complexity crude extracts for improved separations. Toluene, dichloromethane, and ethyl acetate are immiscible with water, and therefore did not extract any water-soluble compounds such as salts and were not believed to extract metabolites from the internal parts of the root to a significant extent. Methanol and acetone, which are miscible with water, resulted in dehydration of root material; the resulting extracts were cloudy and contained some root debris that required filtration prior to purification.

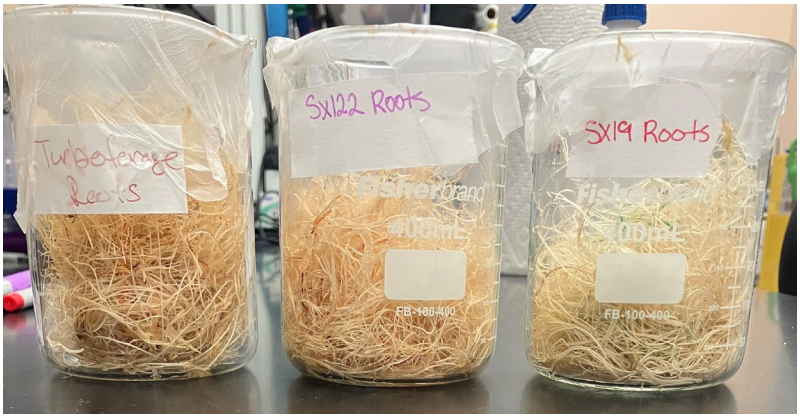

Figure 4. Appearance of freshly harvested roots from Turbo FS, SX-122, and SX-19.

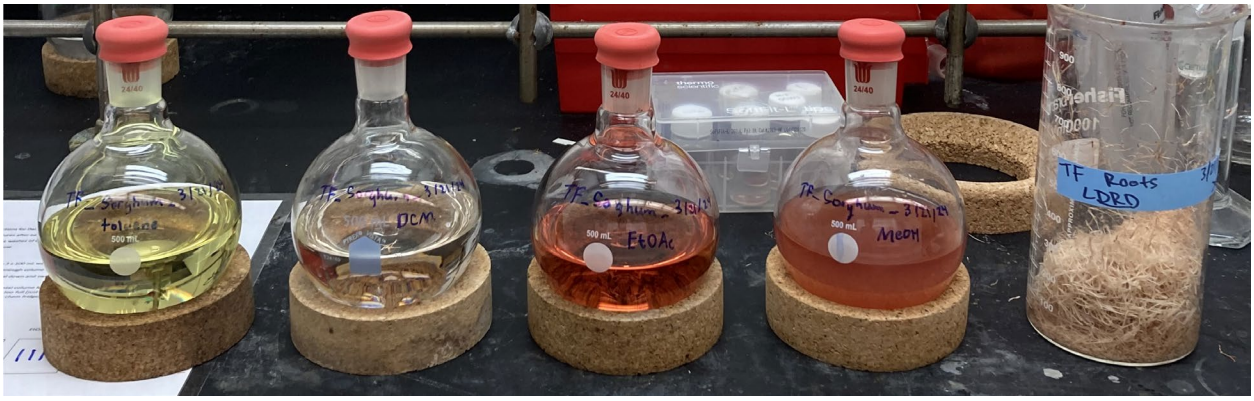

Figure 5. Appearance of Turbo FS root exudate extracts from solvent washes, in order of increasing polarity (from left to right: toluene, dichloromethane, ethyl acetate, methanol; harvested roots).

Roots from SX-122 contained the highest quantities of red compounds, while SX-19 contained the least overall amounts of red compounds. These compounds were moderately polar, with the greatest solubility in MeOH, but limited solubility in either 100% MeOH or 100% water.

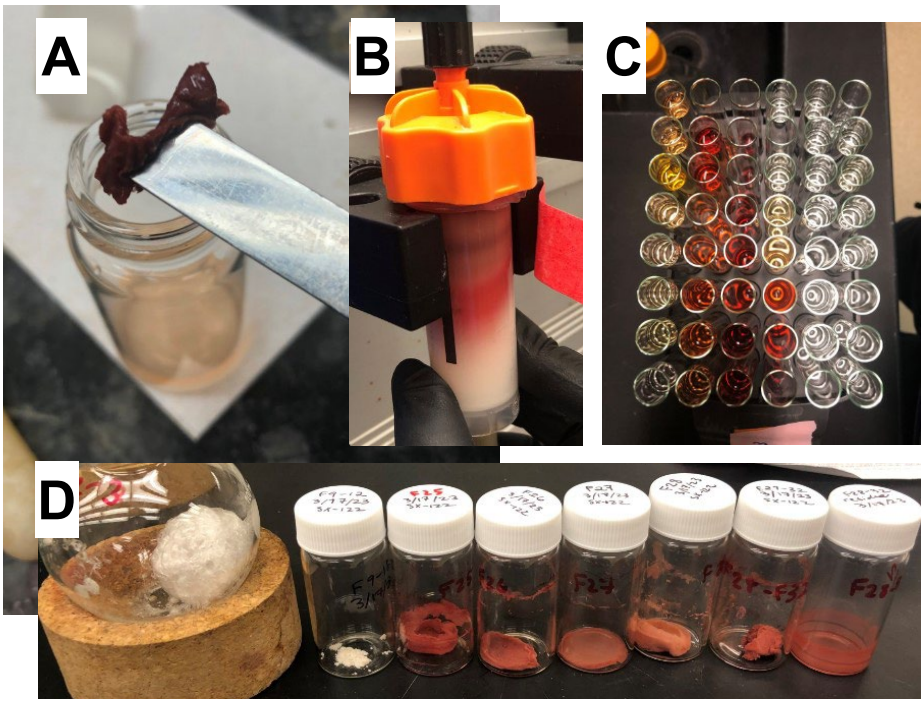

Figure 6. Isolation of red compounds from SX-122 crude exudate, extracted with methanol. (A) Appearance of exudate material as a gummy red solid after rotary evaporation. (B) Reverse phase flash chromatography on C18 silica gel, showing elution of red compounds. (C) Appearance of collected fractions after reverse phase flash chromatography. (D) Appearance of isolated fractions containing red and white solids after lyophilization.

3.2 Fractionation

Certain highly abundant metabolites, such as sorgoleone, the lipid resorcinol, and stigmasterol, could be isolated in high quantities (dozens of milligrams) from root exudates even the lowest resolution purification method, normal phase flash chromatography with the Biotage Isolera.

For more complex mixtures, 2D fractionation (normal phase flash chromatography followed by HPLC into 1 mL volume fractions) yielded the best separations with more pure fractions for crystallization. HPLC fractionation of the “post-sorgoleone peak” fraction from flash chromatography, which eluted as a single peak after sorgoleone at 10% MeOH/DCM from silica gel (Figure 7C), showed ~50 distinct peaks with absorbance at 254 nm (Figure 9). Notably, monitoring absorbance cannot account for non-absorbing compounds that elute, and therefore the HPLC traces shown likely underestimate the complexity of compounds eluting from the column.

Attempts to perform reverse phase HPLC after reverse phase flash chromatography did not yield significant improvement in sample purity for fractions containing red pigments; NMR analyses of these fractions showed even after HPLC, each individual fraction contained a complex mixture of compounds, and improved separations could not be achieved with available resources.

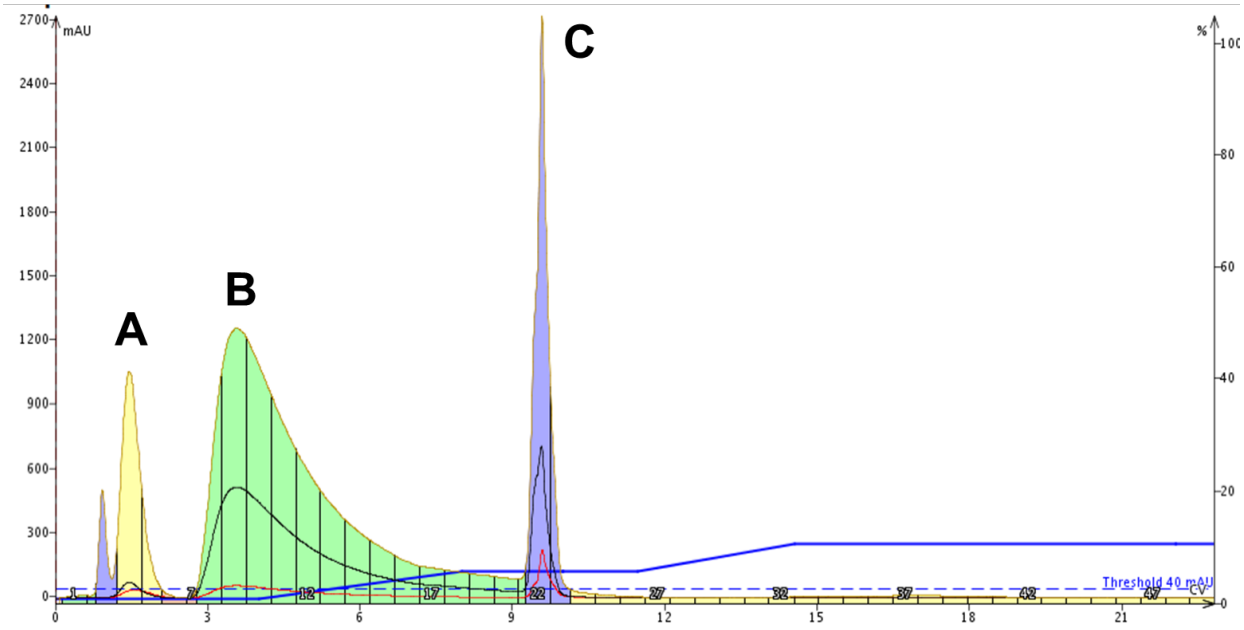

Figure 7. Example of Biotage flash chromatography chromatogram for normal phase separation of chloroform extract of SX-19 over a 0-10% MeOH/DCM gradient. The major UV-absorbing peaks were: (A) lipid resorcinol, (B) sorgoleone, and (C) “post-sorgoleone peak” (complex mixture).

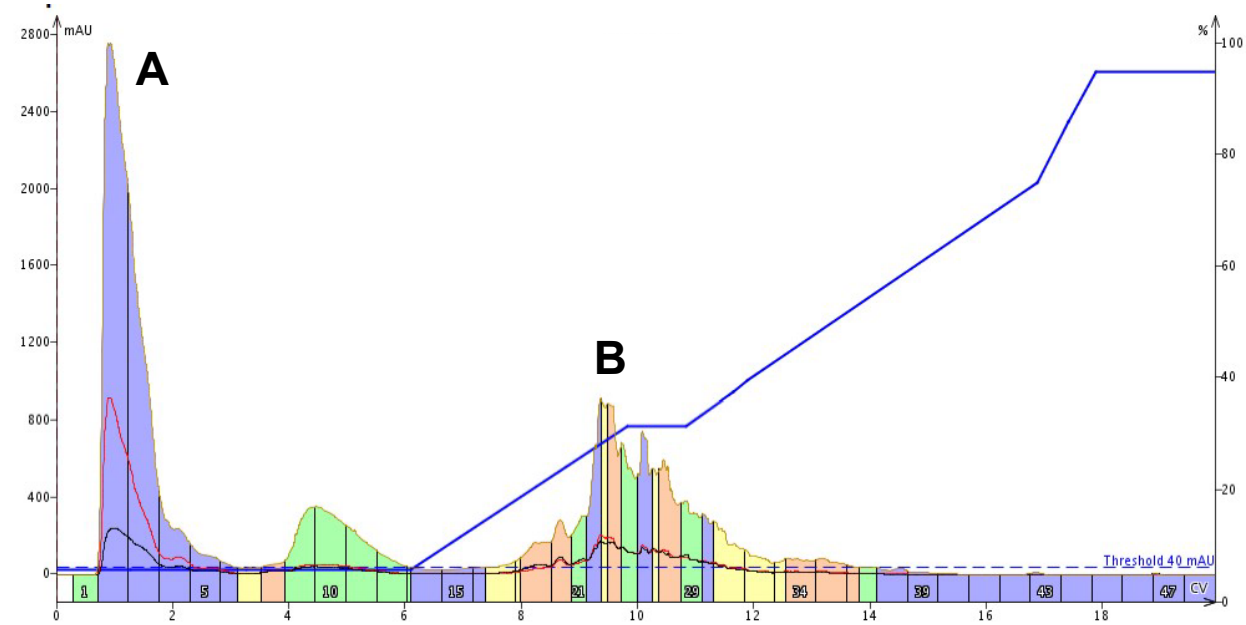

Figure 8. Example of Biotage flash chromatography chromatogram for reverse phase separation of methanol extract of SX-122, eluting 5-95% MeCN/H_2O + 0.1% TFA. The major UV-absorbing peaks were (A) suspected carbohydrates with white appearance when fully dry, hygroscopic, and highly viscous/sticky when wetted and (B) red pigments.

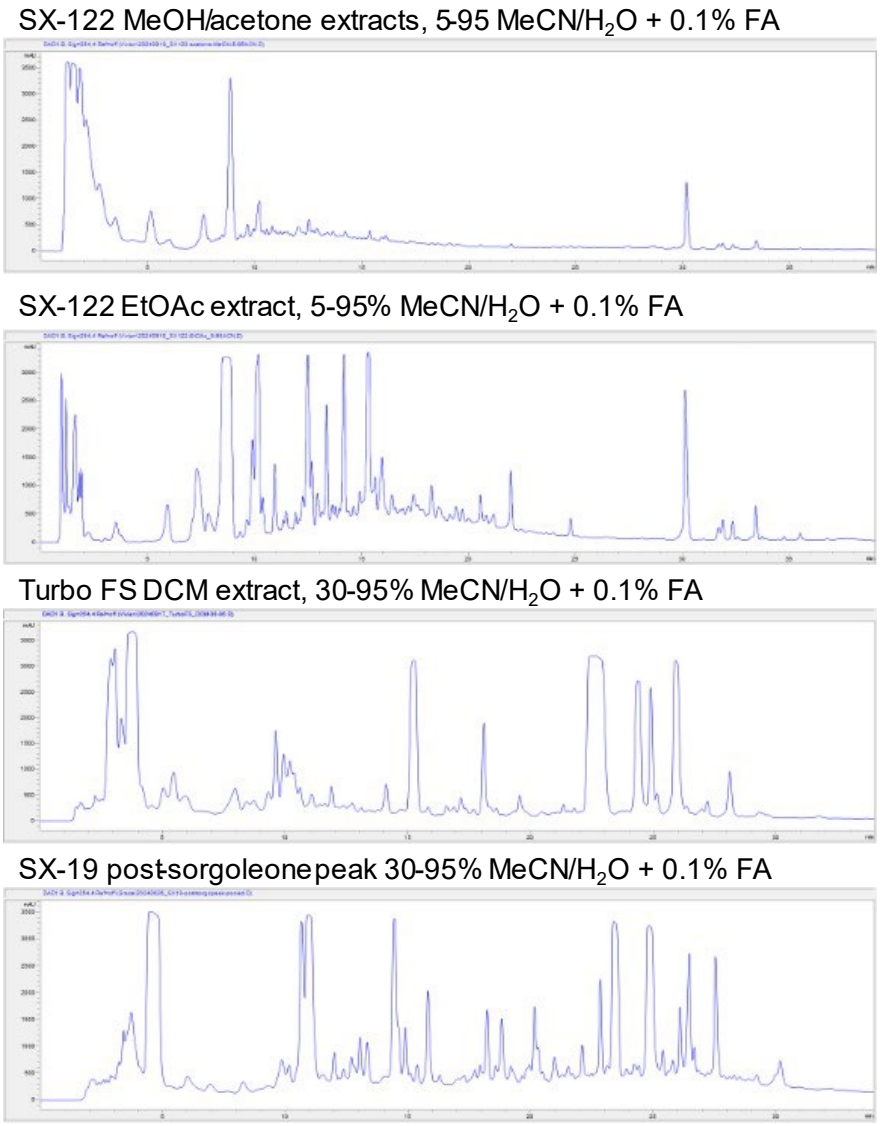

Figure 9. Examples of preparative HPLC chromatograms (absorbance at 254 nm) of different exudate extracts.

3.1 Fraction screening for crystal formation

3.1.1 Manual crystallization from bulk fractions

We transferred fractionated exudates (5-10 mL volumes from flash chromatography or HPLC) into vials or glass test tubes followed by layering with solvents, heating and slow cooling of mixed solvents, or slow evaporation of solvents. Slow evaporation at room temperature was problematic due to microbial growth, particularly in aqueous solvents with minimal amounts of organic solvent and no acid.

While formation of visually crystalline materials was possible for a variety of samples (Figure 10), we observed that frequently, crystals that formed in tubes were challenging to collect and often formed in mixed fractions. Harvesting crystals in the presence of other constituents that

were non-crystalline (e.g. oily) was particularly difficult. Some crystals could be resuspended in a small amount of aqueous or organic solvent, but careful selection of the solvent was needed to avoid redissolving the crystals during this process.

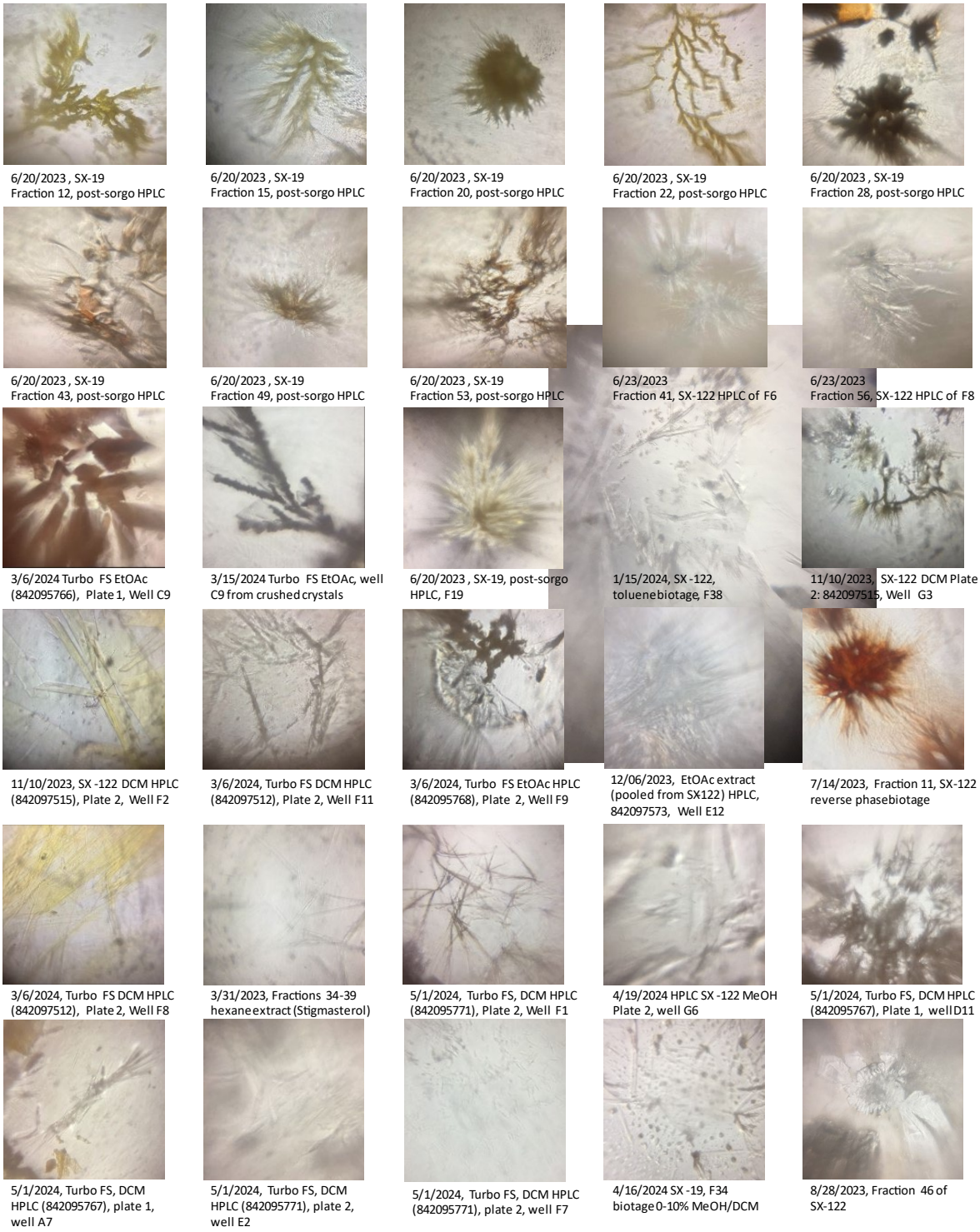

Figure 10. Cellphone microscope images of fractions (3 mm bead objective, 100x magnification) from various fractions from SX-19, SX-122, and Turbo FS sorghum

exudates. All imaged fractions were crystallized and imaged in the bottom of glass test tubes.

3.1.2 Higher throughput crystallization and imaging

ENACT was introduced into our workflow to increase the number of crystallization conditions that could be tested per compound. Crystallization conditions were set up in a 96-well format which allows for future potential automation, further increasing the throughput. The first screens were performed using pure compounds known to be plant metabolites, including some compounds identified in sorghum root exudate metabolomics datasets: salicylic acid, quercetin, naringenin and tricin. Four oils (listed in order of increasing viscosity), Fluorinert FC-40, mineral oil, silicon oil and Fomblin YR-10, were tested, as well as a variety of solvents and concentrations of the compounds being crystallized. The conditions were initially set up at a small scale to minimize sample usage. Once more favorable conditions were found, the condition was scaled up to a volume more amenable for picking up the crystals for TEM grid deposition.

To monitor crystal formation, rather than manually imaging each well using the smartphone camera, we chose a higher-throughput route and employed an Agilent BioTek Cytation C10 Confocal Imaging Reader. To test the imager, we performed bulk crystallization of the 4 pure compounds listed above, and then transferred these to polystyrene glass bottom 96-well plates. After optimizing the imaging settings, we performed ENACT directly in these glass bottom 96-well plates. We determined that the glass Laminex plates used in ENACT publications were incompatible with the reader without creating a custom holder. The 96-well plate (excluding edge wells) could be imaged in approximately 20 min at 4X magnification, providing fast readout of the crystallization results. An example 96-well plate result is shown in Figure 11.

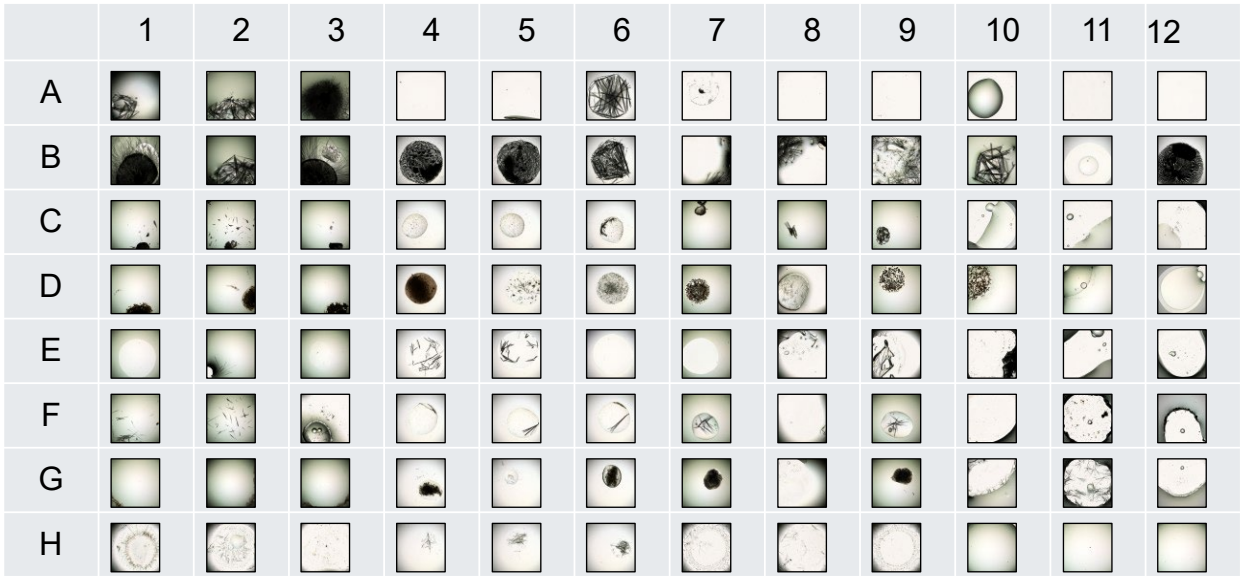

Figure 11. Cytation imaging platform output for 96-well plate containing samples from ENACT crystallization screening of salicylic acid, naringenin, quercetin, and tricin in mineral (columns 1-3), Fluorinert FC-40 (columns 4-6), silicone (columns 7-9), and Fomblin YR-1800 (columns 10-12) oils.

Using the Cytation, results of the ENACT screen were imaged for salicylic acid (Figure 12), quercetin (Figure 13), naringenin (Figure 14) and tricin (Figure 15). In all cases, multiple conditions were found that resulted in crystal formation. Additional imaging of wells or regions of interest was readily performed at higher magnification (up to 40X). Notably, Cytation images at 4X magnification were generally sufficient to differentiate formation of crystalline vs. amorphous solids, such as well C2 compared to well C10 for quercetin (Figure 13).

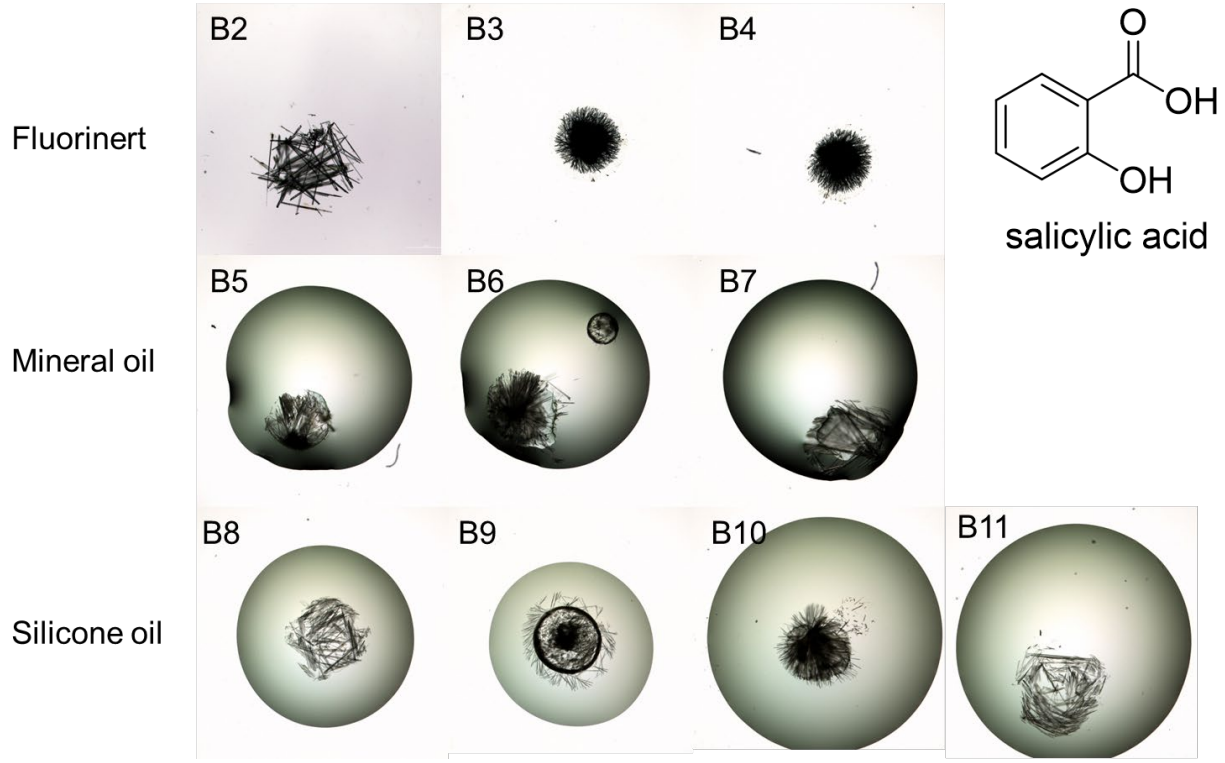

Figure 12. ENACT crystallization screening of salicylic acid (100 mg/mL in 50/50 EtOH/water). Well location is identified in the upper left corner of each image. 4X objective, bright field color.

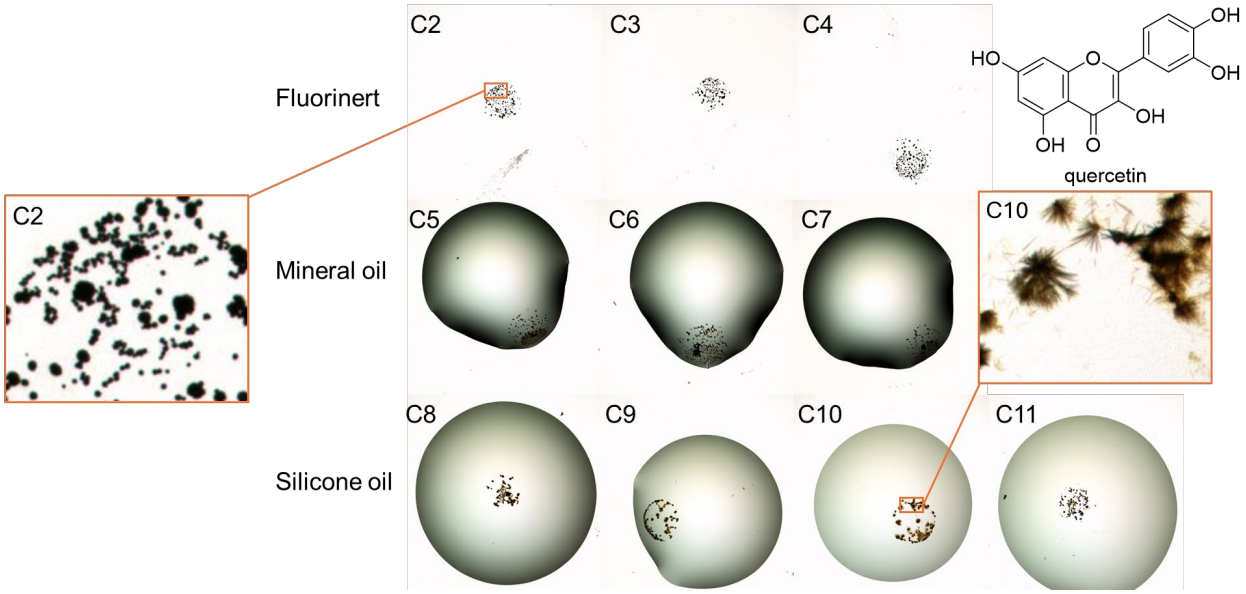

Figure 13. ENACT crystallization screening of quercetin (0.8 mg/mL in 50/50 EtOH/water). Well location is identified in the upper left corner of each image. 4X objective, bright field color. C2 inset shows an example of amorphous solid quercetin compared to C10 insert, which shows formation of quercetin yellow needles.

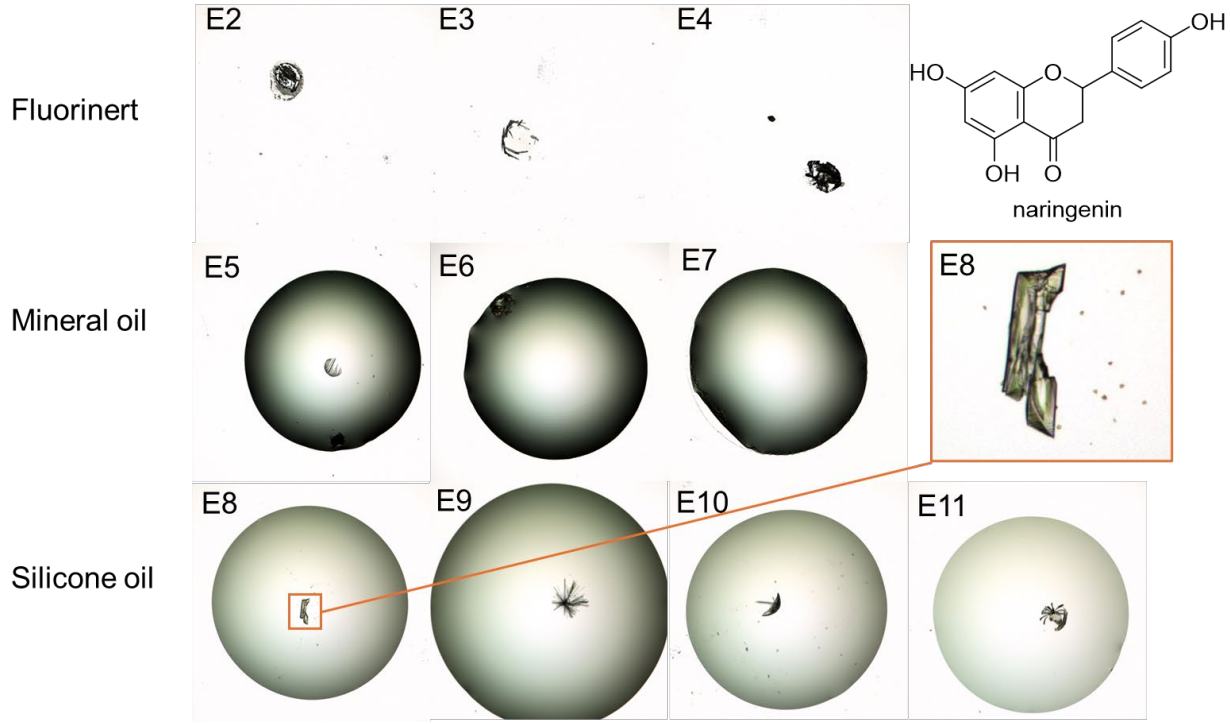

Figure 14. ENACT crystallization screening of naringenin (3.8 mg/mL in 89/11 EtOH/water). Well location is identified in the upper left corner of each image. 4X objective, bright field color.

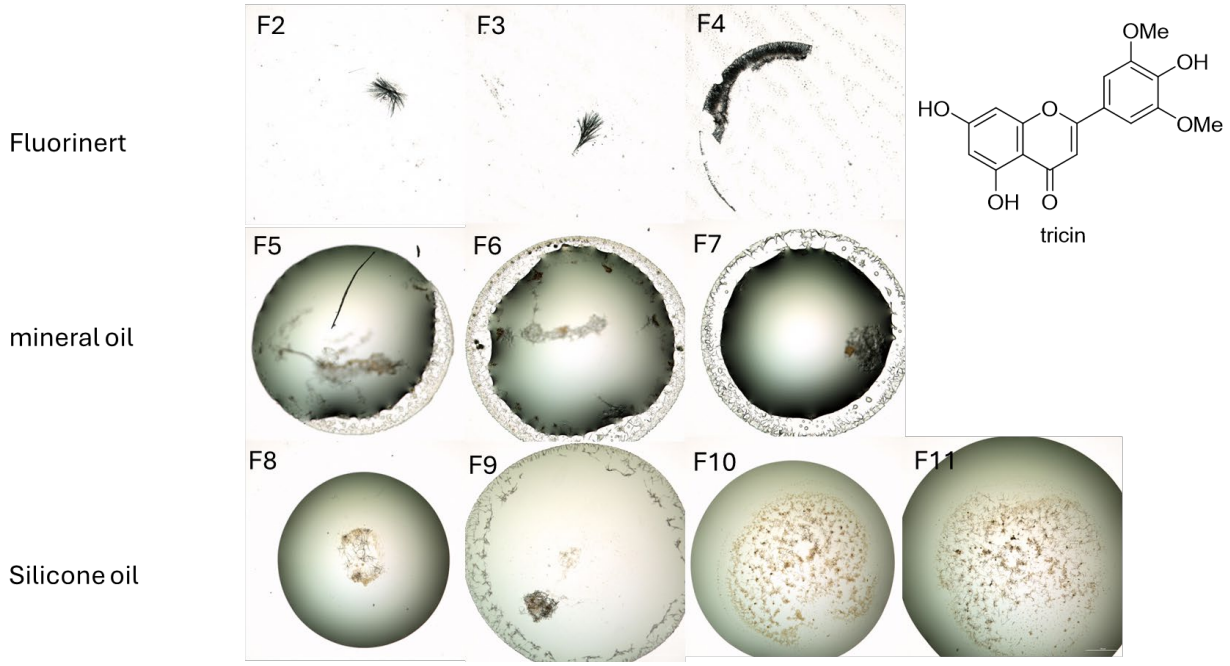

Figure 15. ENACT crystallization screening of tricin (2.8 mg/mL in 100% EtOH). Well location is identified in the upper left corner of each image. 4X objective, bright field color.

Some general trends were observed during ENACT screening. Microbial growth (gray mold) in plates stored at room temperature was observed after 3 or more days, consistent with previous observations of fractions collected in test tubes in mixtures of aqueous and organic solvents. Although crystals were frequently formed in conditions using the most viscous oils (silicone oil and Fomblin), we found that it was difficult to collect the crystals from these drops. The viscosity of the oil created challenges for pipetting samples as well as for blotting oil away while depositing the sample on the TEM grid. High concentrations of oil on a TEM grid are incompatible with MicroED. The least viscous oil (Fluorinert) created a different set of challenges. When applying the oil to the 96-well plate, Fluorinert was too thin, and instead of maintaining a droplet, it would spread out across the well, as can be seen by the lack of a drop in the top row of Figures 11-14. This caused quicker evaporation of the solvent/compound mixture which sometimes still resulted in crystal formation but required the addition of more solvent to lift the crystals off the well and onto a TEM grid. Mineral oil seemed to be the easiest oil to work with, however, fewer crystals formed under this condition with the current compounds tested. An initial investigation of oil removal prior to crystal harvesting, including mechanical removal through careful pipetting or blotting, or washing with an appropriate solvent such as hexane, suggested a combination of these approaches may improve crystal collection in the future. A wider screen of oils and solvents will be necessary to find optimal crystallization and working conditions for the wide diversity of metabolites found in root exudates.

3.2 Metabolite characterization

3.2.1 Sorgoleone-358

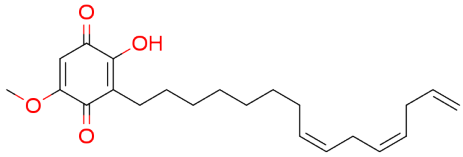

Sorgoleone-358, a known secondary metabolite produced in high quantities by sorghum, was isolated through chloroform extraction from SX-19 roots and purified by flash chromatography as previously described.[13, 14] The identity of sorgoleone-358 was confirmed through NMR and MS. Crystallization of sorgoleone was readily achieved using various mixtures of organic solvents including dichloromethane and methanol, yielding flat yellow plates. In bulk, sorgoleone was a bright orange solid.

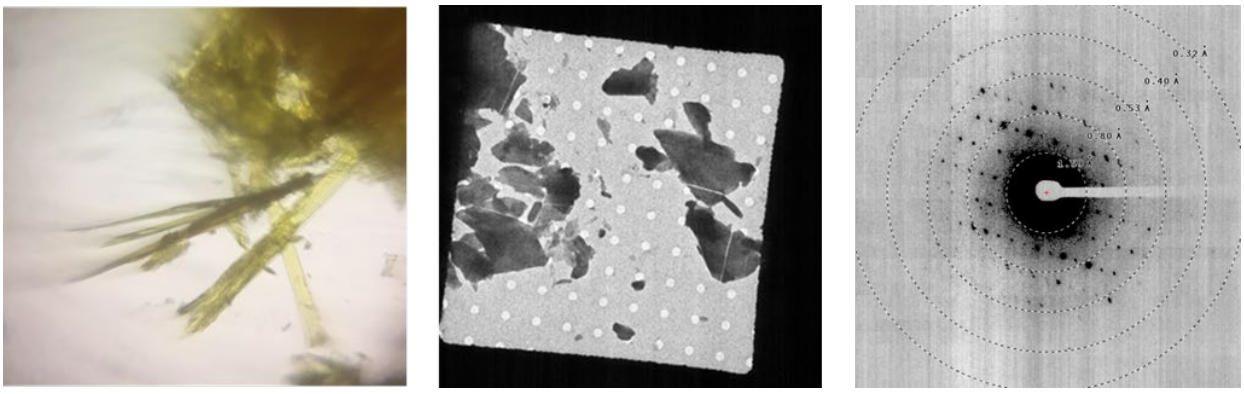

Figure 16. Sorgoleone-358 sample for MicroED analysis. From left to right: smartphone microscope image of crystals, appearance of crystals deposited on TEM grid, and example diffraction pattern.

Sorgoleone-358 crystals (Figure 16A) were broken into smaller pieces and deposited onto TEM grids. Higher mag views showed presence of a lot of material across grid squares (Figure 16B) and the crystals diffracted well out to ~0.5 Å (Figure 16C). More than 50 individual datasets were collected across multiple grids and sample preparations. The head group of sorgoleone-358 was clearly resolved after data processing, the lipid tail however is very flexible, creating high heterogeneity across crystals and datasets. Due to this, we were unable to fully resolve the structure of sorgoleone-358, but we were able to resolve the crystal structure up to C10 of the lipid tail (Figure 17).

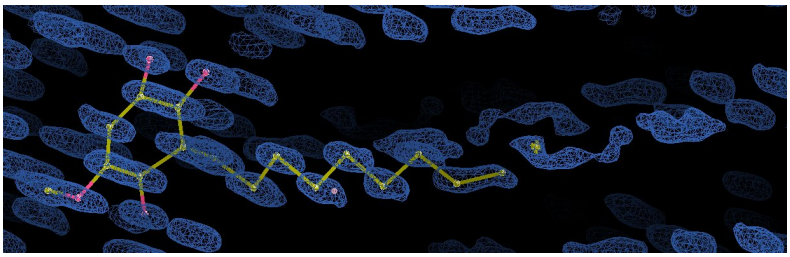

Figure 17. Pymol screenshot of sorgoleone-358 structure up to C10 of the lipid tail (yellow/pink) modeled into the electron density (blue) from MicroED.

3.2.2 Lipid resorcinol

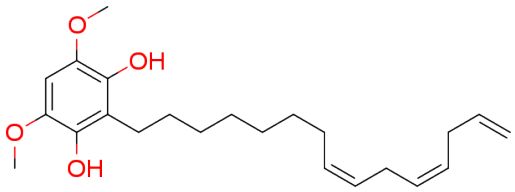

A lipid resorcinol (4,6-dimethoxy-2-[(8‘*Z*,11‘*Z*)-8‘,11‘,14‘-pentadecatriene]resorcinol) with the formula $C_{23}H_{34}O_4$ was isolated in milligram quantities from SX-19. This compound was previously identified in sorghum root exudates by Fate and Lynn in 1996.[15] The biosynthesis of this metabolite proceeds through a similar pathway as sorgoleone, and the compound is structurally similar to sorgoleone-358. This lipid resorcinol is hydrophobic and soluble in nonpolar solvents such as hexane and dichloromethane. It appears as a clear oil in pure form at room temperature. Over time during storage at room temperature or -20 °C, this compound appeared to oxidize and turn brown; an impurity with higher polarity was observed by thin layer chromatography (TLC). The compound identity was confirmed through 1D- and 2D-NMR and HRMS (M+H = 374.25) (Figure 18).

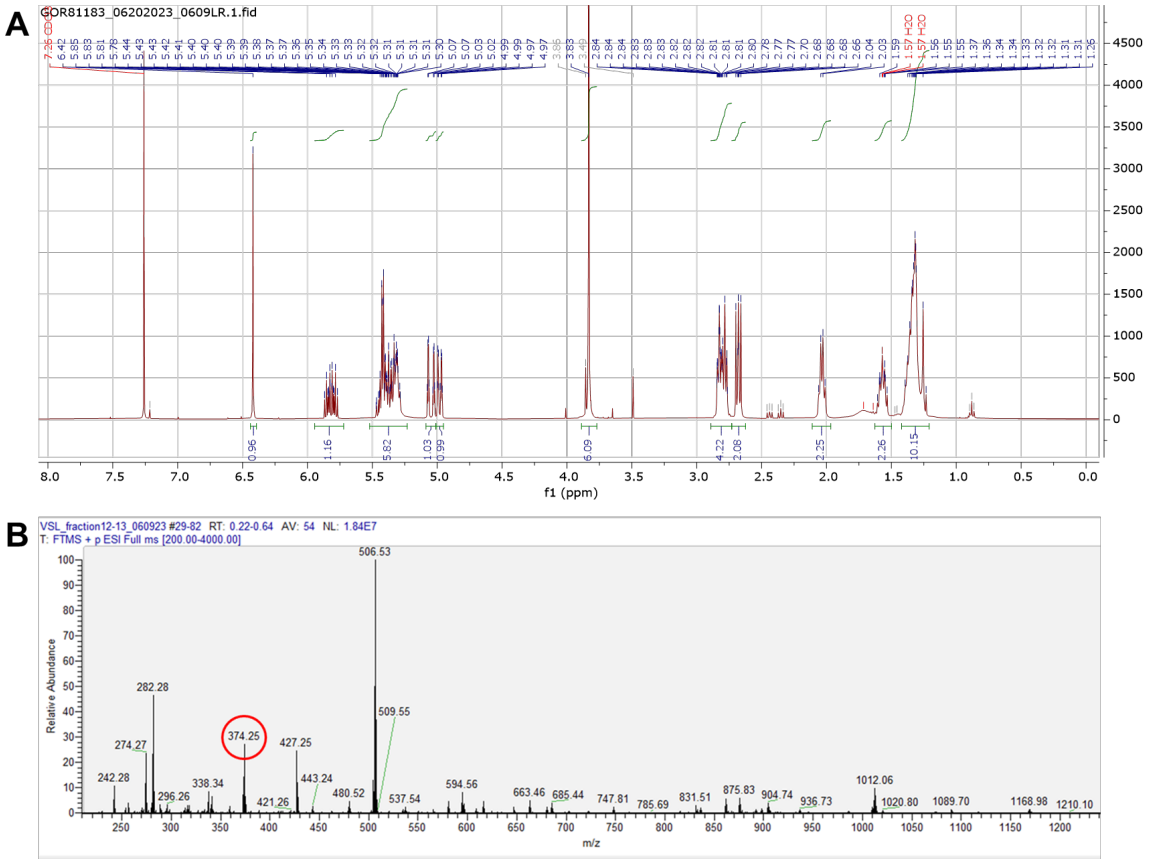

Figure 18. (A) 1H-NMR spectrum in $CDCl_3$ and (B) mass spectrum for lipid resorcinol (4,6-dimethoxy-2-[(8‘*Z*,11‘*Z*)-8‘,11‘,14‘-pentadecatriene]resorcinol) isolated from SX-19 exudates via flash chromatography (hexane/EtOAc).

Notably, the previously published 1H-NMR shifts did not account for all protons in the structure, reporting a total of only 21 protons; we therefore report the structure of this lipid resorcinol compound for the first time with complete NMR shifts: ^{1}H NMR (400 MHz, $CDCl_3$) δ 6.42 (s, 1H), 5.82 (ddt, *J* = 17.2, 10.1, 6.2 Hz, 1H), 5.49 – 5.26 (m, 5H), 5.05 (dq, *J* = 17.1, 1.8 Hz, 1H), 4.98 (dq, *J* = 10.1, 1.6 Hz, 1H), 3.83 (s, 6H), 2.89 – 2.72 (m, 4H), 2.72 – 2.64 (m, 2H), 2.04 (q, *J* = 6.7 Hz, 2H), 1.64 – 1.51 (m, 1H), 1.42 – 1.24 (m, 10H). As this compound was not a solid at room temperature, we could not obtain crystals for MicroED analysis using room temperature crystallization techniques.

3.2.3 Stigmasterol

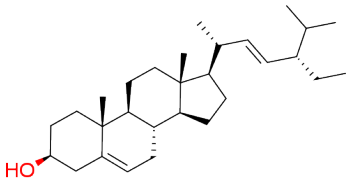

Stigmasterol, a known abundant and hydrophobic plant metabolite that can be found in root exudates,[3] was identified through NMR and HRMS (Figure 19Figure 20). NMR indicated the presence of ~20% beta-sitosterol as an impurity in stigmasterol samples isolated from root exudates.

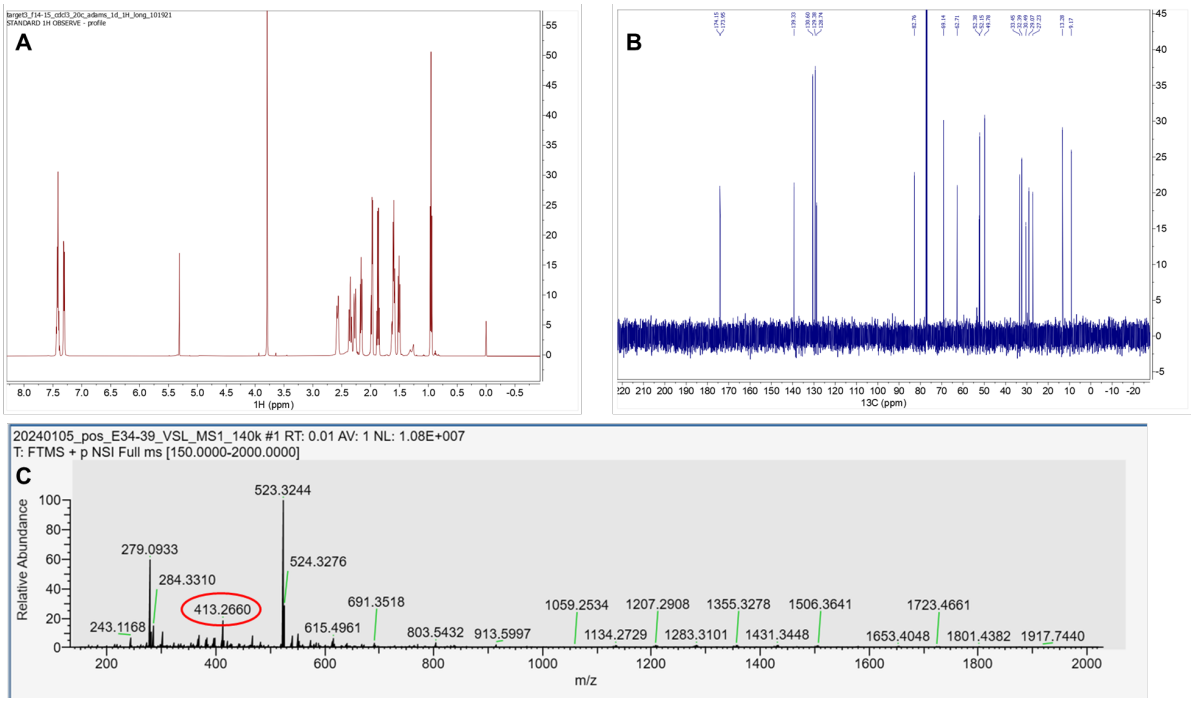

Figure 19. 1D-NMR and MS characterization data for stigmasterol isolated from SX-19 exudates. Approximately 20% beta-sitosterol was also present in these samples. (A) 1H-NMR spectrum. (B) 13C-NMR spectrum. (C) ESI-MS spectrum, positive mode. The M+H peak is indicated in the red circle.

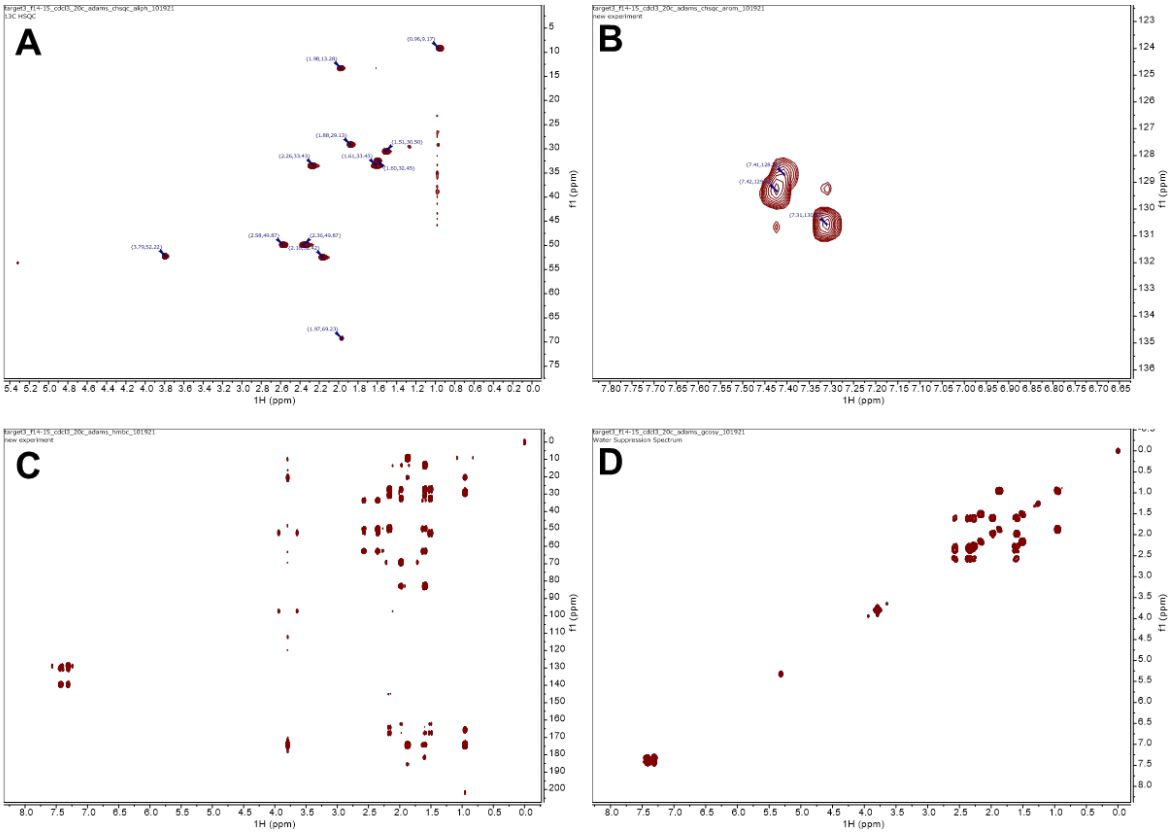

Figure 20. 2D-NMR spectra for stigmasterol isolated from SX-19 exudates. Approximately 20% beta-sitosterol was also present in these samples. (A) Aliphatic 1H-13C HSQC. (B) Aromatic 1H-13C HSQC. (C) 1H-13C HMBC. (D) 1H-1H COSY.

Stigmasterol from sorghum exudates could be recrystallized from hexane and appeared as white/clear needles (Figure 21 left). Deposition of these crystals onto TEM grids (Figure 21 center) followed by MicroED showed that samples diffracted to ~0.5 Å (Figure 21 right) and around 30 datasets were collected. The maximum completeness we were able to achieve after data processing was <75% which was not enough for final structure elucidation. As seen in the center of Figure 21, the crystals on the grid were flat plates and therefore unfortunately had a preferred orientation, creating a large missing wedge of data. Despite multiple attempts to recrystallize the compound in different solvents or to apply the crystals differently on the TEM grids, the issue of preferred orientation persisted.

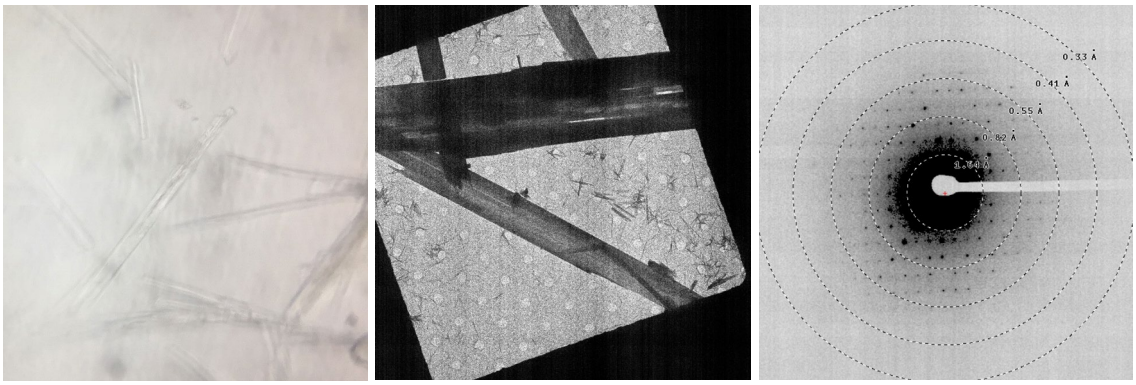

Figure 21. Appearance of stigmasterol crystals isolated from hexane fraction of SX-19 roots and recrystallized from hexane. From left to right: smartphone microscope image of crystals, crystal appearance on TEM grid, and diffraction pattern.

3.2.4 Unknown compounds

Additional crystalline samples were isolated from various root exudate extracts and showed diffraction (Figure 22). Several compounds appeared visually similar to sorgoleone (yellow crystals) but were obtained as separately eluting fractions during HPLC, suggesting some of these may be sorgoleone analogs with different alkyl chain lengths as previously described by the Dayan group.[14] While each of the samples shown in Figure 22 appeared to be crystalline upon visual inspection and showed some diffraction, final structures could not be solved. This was due to a variety of reasons such as weak diffraction, multicrystallinity, preferred orientation, and/or heterogeneity.

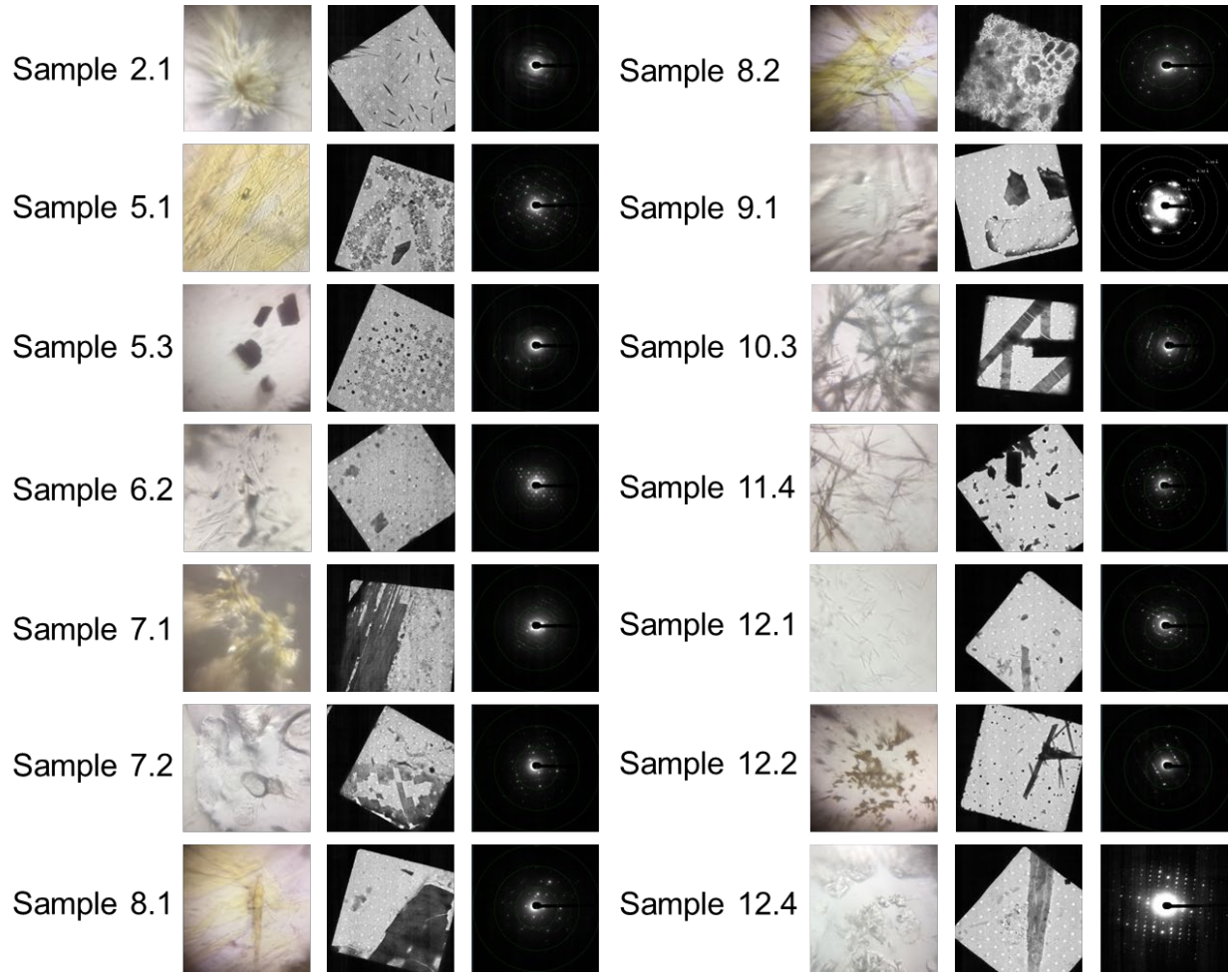

Figure 22. Compiled results for crystalline samples isolated from sorghum root exudate extracts. For each listed sample, from left to right, images show: smartphone microscope image, appearance of crystals on grid, and diffraction pattern.

4.0 Discussion

4.1.1 Exudate isolation

Our initial efforts to obtain sufficiently pure metabolites for chemical characterization and structural elucidation was significantly challenged by the very high complexity of these natural product mixtures. Even though we could routinely obtain 50-100 mg of total crude root exudates from each batch of sorghum root harvest, only a few, highly abundant metabolites could be cleanly isolated through 1D chromatographic techniques.

For example, large amounts of red pigments were obtained from SX-122 root exudates, but no individual compound could be isolated in high purity. Certain types of sorghum are known to produce red pigments in various parts of the plant, including in the root.[16] These compounds have been generally identified as anthocyanidins, which are charged, water soluble pigments; specific anthocyanidins found in sorghum include apigenin, luteolin apigenidin, and luteolinidin. While fractionation of the red pigment material was possible through both reverse phase flash chromatography and HPLC, 1H-NMR analysis of individual HPLC fractions showed each fraction still contained multiple compounds and was highly complex, suggesting alternative methods are needed to obtain higher purity fractions for crystallization. Attempts to crystallize any fractions containing red solids were unsuccessful, yielding amorphous solids or fine precipitates.

In future efforts, 2D-HPLC using two different types of stationary phases may be needed for enhanced separation of metabolites from complex natural samples such as plant root exudates. We obtained the largest number of crystalline compounds using 2D separation, i.e. normal phase flash chromatography of SX-19 chloroform extract followed by reverse phase HPLC of the “post-sorgoleone” fractions that elute immediately after sorgoleone. Alternate types of separation techniques, such as hydrophilic interaction liquid chromatography (HILIC), may also be useful for improving chromatographic resolution of metabolites in root exudates in the future.

4.1.2 Crystallization

Metabolites isolated in high yields from sorghum root exudates (e.g. sorgoleone, stigmasterol) could be bulk recrystallized from various solvents; the ability to obtain these compounds in large quantities also made these samples good candidates for NMR characterization. Although multiple samples were obtained that appeared visually crystalline, low throughput crystallization frequently yielded samples that did not diffract or were multicrystalline. Overall, manual, low throughput methods for crystallization of fractionated material had limited success for generating suitable samples for MicroED, likely due to the high complexity and low abundance of the majority of secondary metabolites in root exudates.

Higher throughput fractionation methods into 96-well plates (1-2 mL volumes), and particularly 2D separations using different types of stationary phases (e.g. SiO_2 normal phase followed by C18 reverse phase), yielded higher purity compounds in lower total quantities. Most fractions were too limited for NMR analysis without extended analysis times, requiring the need for MicroED and crystallization strategies that utilize far less material. Even for fractions that had sufficient material for NMR analysis and were >95% pure by 1H-NMR, manual crystallization through slow evaporation in test tubes yielded crystals that did diffract but were still too poor quality for structural elucidation by MicroED. Thus, we determined that optimization of

crystallization conditions was a necessary next step for improving our overall metabolite identification workflow.

To accomplish this, we employed ENACT for crystallization screening. Samples were set up in a 96-well format, and initial screens required >0.5 µl of a low concentration sample. The first set of screens were set up using known, pure compounds as a proof of concept. Many of the conditions attempted resulted in crystal formation. Further, we observed differences in crystal shape, size, and form across the different crystallization conditions, which could improve MicroED data collection. It is likely that for the sorghum root exudate metabolites, a wider screen of oils, solvents, and/or concentrations would be needed due to high chemical diversity among these compounds. Current efforts are being made to improve the methods for moving the crystals from the 96-well plates and onto TEM grids for MicroED data collection.

4.1.3 MicroED

We have demonstrated that MicroED can be incorporated into the sorghum root exudate metabolite identification pipeline. Many different exudate fractions could be crystallized, as shown by the collection of diffraction patterns for each (Figure 22). Unfortunately, many of the fractions collected had lipid character. As demonstrated with sorgoleone-358, the head group of lipids is more easily resolved than the highly flexible tails. More advanced MicroED data processing methods are likely necessary to fully resolve the structure of these lipid-like samples. Although diffraction data was collected for many other crystalline compounds as well, these compounds were unable to be structurally resolved due to multiple issues. In some case, the initial fractionation did not result in a pure enough sample creating highly heterogeneous crystals, which were difficult to separate out during MicroED data collection and/or data processing. We also ran into the issue of preferred orientation which was often caused by formation of flat plate-like crystals which we were unable to force into different orientations. This resulted in low completion values, preventing us from solving the structure of the compound. Issues of heterogeneity and preferred orientation could potentially be resolved with our higher throughput fractionation strategy, particularly 2D separations, and recent addition of ENACT (see above). With an increase in crystallization screening conditions, this increases the chances of forming crystals of varying size and orientation, which would likely improve MicroED data collection and processing.

4.1.4 Overall workflow and future directions

We established an integrated workflow for metabolite characterization, from crude metabolite generation, fractionation, and chemical structural analysis using various analytical methods. Overall, the application of this workflow to sorghum root exudates, which are highly complex, was very challenging, and successful identification of novel metabolites from these samples will require additional efforts, particularly in the areas of improved separations and crystallization screening. Upgraded instrumentation that allowed for higher throughput sample processing and fractionation—such as an HPLC fraction dispenser adapter tray and new SpeedVac concentrator that enabled sample collection in glass-coated 96-well plates instead of individual glass test tubes—significantly improved our ability to obtain fractions that could crystallize. NMR analysis of isolated fractions containing solid compounds showed substantial improvement in sample purity, yielding multiple fractions that formed crystals that diffracted. We anticipate that further exploration of different fractionation approaches, including different types of chromatography, column and fraction size, and expanded crystallization screening, will improve sample purity and quality. Our most recent results from ENACT screening show that this is a promising direction for MicroED sample generation. Higher throughput technologies such as

automated, nanoliter-scale liquid handling systems will also facilitate more rapid crystallization screening in the future.

This project identified a substantial number of compounds that were poorly crystalline, such as many of the lipid-like, hydrophobic compounds identified in the toluene and DCM extracts. Many of these substances were oily at room temperature, making isothermal crystallization challenging. To improve the identification of these and other poorly crystalline metabolites, additional methods such as crystallization sponges and small molecule crystallization chaperones could be integrated into our overall workflow.[17, 18] We briefly explored tetraaryladamantane crystallization chaperones given their reported high success rate at generating high quality crystals of diverse small molecules, including hydrophobic compounds and compounds that are not solid at room temperature, such as hexane.[19, 20] Crystallization with 1,3,5,7-tetrakis(2,4-dimethoxyphenyl)adamantane (TDA) and 1,3,5,7-tetrakis(2-bromo-4 methoxyphenyl)adamantane (TBro), two commercially available crystallization chaperones, was attempted for sorgoleone and the lipid resorcinol. However, TDA has a working molecular weight range for analytes between 40 and 180 Da, while TBro is reported for hydrophobic analytes between 150 to 270 Da. No reported success of co-crystallization for compounds > 270 Da have been reported for these two chaperones, suggesting they may not be able to accommodate larger metabolites such as sorgoleone, which has a molecular weight of 358 Da. We identified a newer crystallization chaperone in the literature, 1,3,5,7-tetrakis(2-fluoro-4-methoxyphenyl)adamantane (TFM), which was reported to assist the co-crystallization of phytyl acetate, which has a molecular weight of 338 Da.[21] A larger compound, squalene, with a molecular weight of 411 Da, was also co-crystallized with TFM, but the structure could not be fully resolved. Our attempts to synthesize TFM, which is not commercially available, yielded the desired product, but the reaction was lower yielding than reported, and the product was not sufficiently pure to form a solid at room temperature, precluding its use for MicroED testing. Development of alternate crystallization chaperones spanning a wider range of analyte molecular weights and properties may be another promising direction for future technologies that can be integrated with our overall metabolite identification workflow.

5.0 References

1. Canarini A, Kaiser C, Merchant A, Richter A, Wanek W. Root Exudation of Primary Metabolites: Mechanisms and Their Roles in Plant Responses to Environmental Stimuli. Front Plant Sci. 2019;10:157. Epub 20190221. doi: 10.3389/fpls.2019.00157. PubMed PMID: 30881364; PMCID: PMC6407669.

2. Upadhyay SK, Srivastava AK, Rajput VD, Chauhan PK, Bhojiya AA, Jain D, Chaubey G, Dwivedi P, Sharma B, Minkina T. Root Exudates: Mechanistic Insight of Plant Growth Promoting Rhizobacteria for Sustainable Crop Production. Front Microbiol. 2022;13:916488. Epub 20220714. doi: 10.3389/fmicb.2022.916488. PubMed PMID: 35910633; PMCID: PMC9329127.

3. Couvillion SP, Yang IH, Hermosillo D, Eder J, Bell S, Hofmockel KS. Unveiling lipid chemodiversity in root exudates: A comprehensive characterization of the exudate metabo-lipidome in a perennial grass. bioRxiv. 2024:2024.03.22.586263. doi: 10.1101/2024.03.22.586263.

4. Zhang QW, Lin LG, Ye WC. Techniques for extraction and isolation of natural products: a comprehensive review. Chin Med. 2018;13:20. Epub 20180417. doi: 10.1186/s13020-018-0177-x. PubMed PMID: 29692864; PMCID: PMC5905184.

5. Lopes NP, Roberto da Silva R. From structural determination of natural products in complex mixtures to single cell resolution: Perspectives on advances and challenges for mass spectrometry. Frontiers in Natural Products. 2023;2. doi: 10.3389/fntpr.2023.1109557.

6. Wishart DS, Sayeeda Z, Budinski Z, Guo A, Lee BL, Berjanskii M, Rout M, Peters H, Dizon R, Mah R, Torres-Calzada C, Hiebert-Giesbrecht M, Varshavi D, Varshavi D, Oler E, Allen D, Cao X, Gautam V, Maras A, Poynton EF, Tavangar P, Yang V, van Santen JA, Ghosh R, Sarma S, Knutson E, Sullivan V, Jystad AM, Renslow R, Sumner LW, Linington RG, Cort JR. NP-MRD: the Natural Products Magnetic Resonance Database. Nucleic Acids Res. 2022;50(D1):D665-D77. doi: 10.1093/nar/gkab1052. PubMed PMID: 34791429; PMCID: PMC8728158.

7. Shi D, Nannenga BL, Iadanza MG, Gonen T. Three-dimensional electron crystallography of protein microcrystals. Elife. 2013;2:e01345. Epub 20131119. doi: 10.7554/eLife.01345. PubMed PMID: 24252878; PMCID: PMC3831942.

8. Ghosh R, Bu G, Nannenga BL, Sumner LW. Recent Developments Toward Integrated Metabolomics Technologies (UHPLC-MS-SPE-NMR and MicroED) for Higher-Throughput Confident Metabolite Identifications. Front Mol Biosci. 2021;8:720955. Epub 20210902. doi: 10.3389/fmolb.2021.720955. PubMed PMID: 34540897; PMCID: PMC8445028.

9. Delgadillo DA, Burch JE, Kim LJ, de Moraes LS, Niwa K, Williams J, Tang MJ, Lavallo VG, Khatri Chhetri B, Jones CG, Rodriguez IH, Signore JA, Marquez L, Bhanushali R, Woo S, Kubanek J, Quave C, Tang Y, Nelson HM. High-Throughput Identification of Crystalline Natural Products from Crude Extracts Enabled by Microarray Technology and microED. ACS Cent Sci. 2024;10(1):176-83. Epub 20231220. doi: 10.1021/acscentsci.3c01365. PubMed PMID: 38292598; PMCID: PMC10823509.

10. Tyler AR, Ragbirsingh R, McMonagle CJ, Waddell PG, Heaps SE, Steed JW, Thaw P, Hall MJ, Probert MR. Encapsulated Nanodroplet Crystallization of Organic-Soluble Small Molecules. Chem. 2020;6(7):1755-65. Epub 20200709. doi: 10.1016/j.chempr.2020.04.009. PubMed PMID: 32685768; PMCID: PMC7357602.

11. Hollerbach AL, Ibrahim YM, Lin VS, Schultz KJ, Huntley AP, Armentrout PB, Metz TO, Ewing RG. Identification of Unique Fragmentation Patterns of Fentanyl Analog Protomers Using Structures for Lossless Ion Manipulations Ion Mobility-Orbitrap Mass Spectrometry. J Am Soc Mass Spectrom. 2024;35(4):793-803. Epub 20240312. doi: 10.1021/jasms.4c00049. PubMed PMID: 38469802.

12. Powell SM, Novikova IV, Kim DN, Evans JE. AutoMicroED: A semi-automated MicroED processing pipeline. bioRxiv. 2021:2021.12.13.472146. doi: 10.1101/2021.12.13.472146.

13. Van Fossen EM, Kroll JO, Anderson LN, McNaughton AD, Herrera D, Oda Y, Wilson AJ, Nelson WC, Kumar N, Frank AR, Elmore JR, Handakumbura P, Lin VS, Egbert RG. Profiling sorghum-microbe interactions with a specialized photoaffinity probe identifies key sorgoleone binders in Acinetobacter pittii. Appl Environ Microbiol. 2024:e0102624. Epub 20240909. doi: 10.1128/aem.01026-24. PubMed PMID: 39248464.

14. Kagan IA, Rimando AM, Dayan FE. Chromatographic separation and in vitro activity of sorgoleone congeners from the roots of sorghum bicolor. J Agric Food Chem. 2003;51(26):7589-95. doi: 10.1021/jf034789j. PubMed PMID: 14664512.

15. Fate GD, Lynn DG. Xenognosin Methylation Is Critical in Defining the Chemical Potential Gradient That Regulates the Spatial Distribution in Striga Pathogenesis. Journal of the American Chemical Society. 1996;118(46):11369-76. doi: 10.1021/ja961395i.

16. Balasubramanian VK, Dampanaboina L, Cobos CJ, Yuan N, Xin Z, Mendu V. Induced secretion system mutation alters rhizosphere bacterial composition in Sorghum bicolor (L.) Moench. Planta. 2021;253(2):33. Epub 20210118. doi: 10.1007/s00425-021-03569-5. PubMed PMID: 33459875; PMCID: PMC7813745.

17. Li H, Li Y, Jiao J, Lin C. Recent research progress on crystallization strategies for difficult-to-crystallize organic molecules. Results in Chemistry. 2023;5. doi: 10.1016/j.rechem.2023.100859.

18. Metherall JP, Carroll RC, Coles SJ, Hall MJ, Probert MR. Advanced crystallisation methods for small organic molecules. Chem Soc Rev. 2023;52(6):1995-2010. Epub 20230320. doi: 10.1039/d2cs00697a. PubMed PMID: 36857636.

19. Krupp F, Frey W, Richert C. Absolute Configuration of Small Molecules by Co-Crystallization. Angew Chem Int Ed Engl. 2020;59(37):15875-9. Epub 20200629. doi: 10.1002/anie.202004992. PubMed PMID: 32441841; PMCID: PMC7540501.

20. Rami F, Nowak J, Krupp F, Frey W, Richert C. Co-crystallization of an organic solid and a tetraaryladamantane at room temperature. Beilstein J Org Chem. 2021;17:1476-80. Epub 20210621. doi: 10.3762/bjoc.17.103. PubMed PMID: 34239614; PMCID: PMC8239258.

21. Berking T, Hartenfels J, Lenczyk C, Santiso-Quinones G, Frey W, Richert C. A Fluorinated Chaperone Gives X-ray Crystal Structures of Acyclic Natural Product Derivatives up to 338 Molecular Weight. Angew Chem Int Ed Engl. 2024;63(27):e202402976. Epub 20240529. doi: 10.1002/anie.202402976. PubMed PMID: 38709597.

Pacific Northwest National Laboratory

902 Battelle Boulevard
P.O. Box 999
Richland, WA 99354

1-888-375-PNNL (7665)

www.pnnl.gov